AD-A130 985 JOINT SERVICES ELECTRONICS PROGRAM(U) HARVARD UNIV 1/1
CAMBRIDGE MA DIV OF APPLIED SCIENCES N BLOEMBERGEN
01 APR 83 N00014-75-C-0648

UNCLASSIFIED F/G 9/5 NL

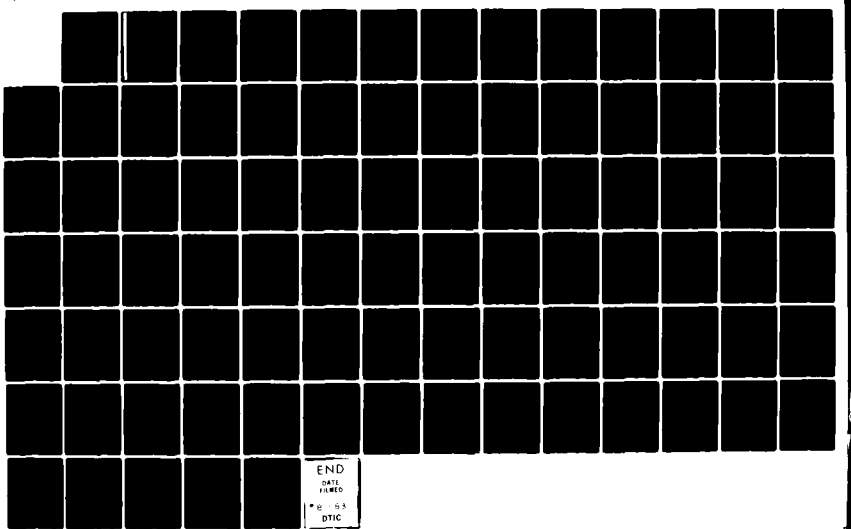

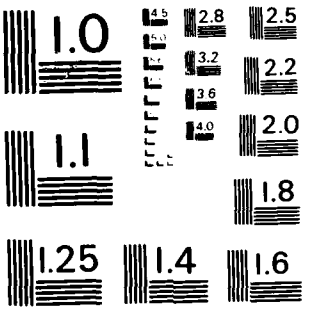

(12)

Division of Applied Sciences
Harvard University Cambridge, Massachusetts

ANNUAL PROGRESS REPORT NO. 96

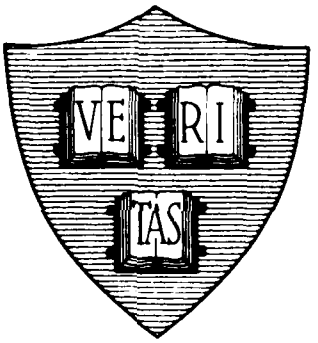

JOINT SERVICES ELECTRONICS PROGRAM

N00014-75-C-0648

Covering Period
April 1, 1982 - March 31, 1983

April 1983

Joint Services Electronics Program
N00014-75-C-0648

ANNUAL PROGRESS REPORT NO. 96

Covering Period

April 1, 1982 - March 31, 1983

The research reported in this document, unless otherwise indicated, was made possible through support extended to the Division of Applied Sciences, Harvard University by the U. S. Army Research Office, the U. S. Air Force Office of Scientific Research and the U. S. Office of Naval Research under the Joint Services Electronics Program by Contract N00014-75-C-0648. Related research sponsored by the Office of Naval Research, the National Science Foundation, the National Aeronautics and Space Administ ation, and by the University is also reported briefly with appropriate acknowledgement.

Division of Applied Sciences

Harvard University

Cambridge, Massachusetts

UNCLASSIFIED

SECURITY CLASSIFICATION OF THIS PAGE *(When Data Entered)*

REPORT DOCUMENTATION PAGE		READ INSTRUCTIONS BEFORE COMPLETING FORM
1. REPORT NUMBER Annual Progress Report No. 96	2. GOVT ACCESSION NO. A130 983	3. RECIPIENT'S CATALOG NUMBER
4. TITLE *(and Subtitle)* Joint Services Electronics Program Progress Report		5. TYPE OF REPORT & PERIOD COVERED Annual April 1, 1982-March 31,1983
		6. PERFORMING ORG. REPORT NUMBER Report No. 96
7. AUTHOR(s) N. Bloembergen		8. CONTRACT OR GRANT NUMBER(s) N00014-75-C-0648
9. PERFORMING ORGANIZATION NAME AND ADDRESS Division of Applied Sciences Harvard University Cambridge, MA 02138		10. PROGRAM ELEMENT, PROJECT, TASK AREA & WORK UNIT NUMBERS
11. CONTROLLING OFFICE NAME AND ADDRESS Office of Naval Research 800 N. Quincy St. Arlington, VA 22217		12. REPORT DATE 1 April 1983
		13. NUMBER OF PAGES 86
14. MONITORING AGENCY NAME & ADDRESS*(if different from Controlling Office)*		15. SECURITY CLASS. *(of this report)* Unclassified
		15a. DECLASSIFICATION/DOWNGRADING SCHEDULE

16. DISTRIBUTION STATEMENT *(of this Report)*

17. DISTRIBUTION STATEMENT *(of the abstract entered in Block 20, if different from Report)*

Approved for public release; distribution unlimited.

18. SUPPLEMENTARY NOTES

19. KEY WORDS *(Continue on reverse side if necessary and identify by block number)*

Solid state electronics, quantum electronics, information and control electronics, optimization, electromagnetic phenomena

20. ABSTRACT *(Continue on reverse side if necessary and identify by block number)*

An annual report of the JSEP (Joint Services Electronic Program) in solid state electronics, quantum electronics, information electronics control and optimization and electromagnetic phenomenon is presented. Results of the research to date are summarized and significant accomplishments are discussed.

DD FORM 1 JAN 73 1473 EDITION OF 1 NOV 65 IS OBSOLETE
S/N 0102-014-6601

UNCLASSIFIED

SECURITY CLASSIFICATION OF THIS PAGE *(When Data Entered)*

ANNUAL PROGRESS REPORT NO. 96

Joint Services Contract

N00014-75-C-0648	The Steering Committee

Related Contracts

N00014-79-C-0419	T.T. Wu
N00014-79-C-0776	Y.C. Ho
N00014-83-K-0030	N. Bloembergen, F. Spaepen
F29-601-81-K-0010	T.T. Wu
NSF-ECS-81-21428	R. Brockett
NSF-ECS-82-13680	Y.C. Ho
NSF-DMR-79-04155	M. Tinkham
NSF-DMR-80-20247	H. Ehrenreich, P.S. Pershan, M. Tinkham
NSF-DMR-82-07431	H. Ehrenreich
NSF-DMR-82-12189	P.S. Pershan
NSF-DMR-82-05147	M. Tinkham
NSF-DMR-81-08327	W. Paul
NSF-PHY-82-07080	T.W. Mossberg
DAAG29-81-K-0071	N. Bloembergen
DAAG29-83-K-0027	R. Brockett
DAAG29-83-K-0050	T.W. Mossberg
DOE-DE-AC02-82ER12064	W. Paul
DOE-DE-AS02-76ER03227	T.T. Wu
DOE-XW-0-9358-1	W. Paul
AFOSR-81-0054	R. Brockett
SERI-XB-2-02144-1	W. Paul
ERDA-EY-76-S-02-3227	T.T. Wu
Draper Lab. DL-H-208109	Y.C. Ho
Sandia National Lab. 68-0404	T.T. Wu

JOINT SERVICES ELECTRONICS PROGRAM

April 1, 1982 - March 31, 1983

ADMINISTRATIVE STAFF

Contract

N00014-75-C-0648

The Steering Committee

Prof. N. Bloembergen
Prof. R.W. Brockett
Prof. H. Ehrenreich
Prof. Y.C. Ho
Prof. T.W. Mossberg
Prof. W. Paul
Prof. P.S. Pershan
Prof. R. Suri
Prof. M. Tinkham
Prof. R.M. Westervelt
Prof. T.T. Wu
Dr. P. McKinney
Dr. L. Strong

RESEARCH STAFF

Dr. R. Bansal (summer)
Dr. J.T. deBettencourt
Dr. N. Bloembergen
Dr. G.E. Blonder (till 8/82)
Dr. R.W. Brockett
Dr. I. Burak
Dr. C.I. Byrnes
Dr. N.W. Carlson
Dr. T.S. Chang
Dr. C.D. Cordero
Dr. P. Crouch
Dr. H. Ehrenreich
Dr. D.J. Frank (till 11/82)
Dr. F. Habbal (till 11/15/82)
Dr. Y.C. Ho
Dr. R.W.P. King
Dr. P.B. Kirby
Dr. T.M. Klapwijk (visitor)
Dr. H. Kurz
Dr. A. Lachter
Dr. C. Lee
Dr. H.-M. Lee (till 8/82)
Dr. C.J. Lobb
Dr. L.A. Lompre
Dr. E. Mazur
Dr. T.W. Mossberg
Dr. M. Octavio (visitor, fall 1982)
Dr. S. Oguz
Dr. W. Paul
Dr. P.S. Pershan
Dr. B. von Roedern
Dr. L. Sorenson
Dr. R. Suri
Dr. M. Tinkham
Dr. B. Tolwinski
Dr. A. Weiss
Dr. T.T. Wu
Dr. B.G. Yacobi

INTRODUCTION

This report covers progress made in the period 1 April, 1982 to 31 March, 1983 for the ten research units funded under the Joint Services Electronics Program at Harvard University. It is broken down into four major divisions of electronic research--solid state electronics, quantum electronics, information electronics control and optimization and electromagnetic phenomena. It also includes a report of Significant Accomplishments which contains the most noteworthy results of all research units contributing to the JSEP program at Harvard. This section contains: the Submillimeter-Wave Properties of Small-area Tunnel Junctions by research unit 2; Nonequilibrium Switching Phenomena on Picosecond Time Scales by research unit 2; Liquid Crystal X-Ray Mirror by research unit 4 and the Rhombic Simulator as a Model for the Theoretical and Experimental Study of Large Scale EMP Simulators under CW and Pulse Excitation by research unit 10. These significant accomplishment reports are not duplicated in other sections of the Annual Report where other activities funded under the same research unit are described.

CONTENTS

rapidly to zero and the normal voltage appears. Our detailed numerical computer solutions of the Schmid-Schön equations[3] for nonequilibrium superconductors, or our own simpler analytical models,[4] predict these various features, and our measurements provide the first measurements with sufficient voltage sensitivity and time resolution to observe anything beyond the simple time delay till full normal voltage appears. There is generally satisfactory semiquantitative agreement, which not only confirms the theoretical ideas but also yields a new measurement of the characteristic relaxation times in Al and In, the two metals studied in detail. Several publications are currently in preparation to report this work in the literature.

References

1. S.M. Faris, *Appl. Phys. Lett.* 36, 1005 (1980).

2. D.J. Frank, "Transient Response of Superconducting Microbridges to Supercritical Currents," Ph.D. Thesis, Physics Department, Harvard University, November, 1982.

3. A. Schmid, G. Schön, and M. Tinkham, *Phys. Rev.* B21, 5076 (1980).

4. M. Tinkham, chapter in *Nonequilibrium Superconductivity, Phonons, and Kapitza Boundaries*, K.E. Gray, Ed., NATO ASI B65, Plenum, New York, (1981), p. 231.

V.3 A Liquid Crystal X-Ray Mirror. P.S. Pershan; Research Unit 4, SOLID STATE ELECTRONICS.

The flat horizontal interface between a fluid smectic-A liquid crystal and air was shown to act as a highly reflecting mirror for X-rays that are incident at ~1.5 degrees from the surface. The experiment was carried out at the German synchrotron facility DESY (HASYLAB) in collaboration with

Dr. Jens Als-Nielsen of the Risø National Laboratory in Denmark. Molecules at the surface of the higher temperature nematic phase align themselves normal to the surface in such a way as to produce a layered structure. As the temperature is lowered the number of layers grows until one reaches the transition temperature between the nematic and smectic-A phase. At that point the entire sample consists of nearly parallel layers that are all nearly parallel to the free surface. Synchrotron X-ray studies reveal a mosaic distribution of layer normals less than .02 degrees. Bragg reflection from this multilamellar array of smectic layers is extremely intense.

Initial discovery of this effect was carried out using the liquid crystal 80CB. It must be kept horizontal because of the highly fluid nature of the smectic-A phase. Further experiments were carried out in Denmark in collaboration with the Danish group on a second liquid crystal 40.8 that has a lower temperature solid or "smectic-B" phase in which the surface can be reoriented. The particular interest of the liquid crystals are that their lattice spacings, from 25-30 Å, make them excellent candidates for use as X-ray mirrors for soft X-rays (200-1200 eV). Furthermore, the relative softness of the liquid crystal, even in the solid phase, holds out some promise of bending the mirror to achieve some degree of focussing.

V.4 The Rhombic Simulator as a Model for the Theoretical and Experimental Study of Large-Scale EMP Simulators under CW and Pulse Excitation. T.T. Wu, R.W.P. King, and H.M. Shen; Research Unit 10, ELECTROMAGNETIC PHENOMENA.

Very large parallel-plate type structures with tapered input and output ends are used to test the vulnerability of aircraft and missiles to electromagnetic pulses that are supposed to simulate those emanating from nuclear plosions the atmosphere. Voltage pulses applied at one end of the

structure excite current pulses that spread out and travel along the wire-mesh walls, continuously generating a transient electromagnetic field between them. An aircraft under test and located in the 'working volume' of a simulator is exposed to a field that is much more complicated than that generated in the absence of the test obstacle because of multiple reflections between the obstacle and the walls of the simulator. How useful are such tests if the electromagnetic fields acting to induce currents and charges on the skin of the aircraft or missile differ significantly from those characteristic of the radiation from a nuclear explosion in the air?

Extensive measurements in the Harvard model simulator over a wide range of frequencies have shown[1,2] that transmission-line theory, which had been used to design the tapered parallel-plate type of simulator, is completely inadequate to determine its properties except at very low frequencies. At the middle and higher frequencies, the currents in the walls of the simulator and the fields between them are governed by radiation--which is ignored in transmission-line theory. A theory that takes full account of radiation is required.

In order to gain an understanding of the basic physical principles that underlie the high-frequency and pulse operation of a traveling-wave simulator, it was necessary to simplify its structure so that it could be analyzed in general and not only under low-frequency conditions. The configuration selected is a thin-wire, double-rhombic antenna, the conductors of which, in effect, lie along the edges of a volume like that occupied by a wire-mesh or metal-plate simulator. Since the currents that generate the electromagnetic field in the working volume are all localized in electrically thin conductors, their distributions can be determined accurately and from them the field for all relevant frequencies. The rhombic simulator has been analyzed theoretically

in the frequency domain,[3] the theory has been verified experimentally,[4] and all important properties have been compared with the corresponding ones of a parallel-plate simulator.[4] The results indicate that the rhombic simulator has characteristics that are very similar and generally superior to those of the comparable parallel-plate simulator in the low, intermediate, and high frequency ranges. Most important, these properties can be determined analytically so that their origin is understood. This includes the so-called 'notch' phenomenon.

A comprehensive experimental[5] and theoretical[6] study has been made of the rhombic simulator when excited by a voltage pulse at the driving point. The associated current pulses that travel along the conducting tubes have been measured and calculated together with the complicated sequences of pulses that characterize the electromagnetic field in the working volume between the wires. These include the incident pulse and the pulses reflected from the load and other points. It has been shown that the transient electromagnetic field is readily understood in terms of the fields radiated by a set of subpulses in the successive segments of the rhombic wires traversed by the current. Of particular importance are the relative time delays in the sequence of the subpulses. Corresponding experiments on the pulse-excited parallel-plate simulator[7] have yielded results that are readily interpreted in terms of similar effects on the now well-understood rhombic simulator.

The complete theoretical and experimental understanding of the complicated physical phenomena associated with the transient electromagnetic field in a rhombic EMP simulator is a significant accomplishment in basic electromagnetic theory. This advance has been enhanced further by the derivation of a new solution of the integral equation for the current in a cylindrical conductor

in the time domain.[8] The demonstration that the rhombic and conventional parallel-plate simulators have similar properties is of practical importance in that it provides a means for the systematic evaluation and possible improvement of conventional simulators. The basic theory and experimental procedure are also provided for the definitive study of the crucial obstacle--simulator interaction.

References

1. R.W.P. King and D.J. Blejer, "The Electromagnetic Field in an EMP Simulator at a High Frequency," *IEEE Trans. Electromagn. Compatibil.*, EMC-21, 263-269, August 1979.

2. R.W.P. King, D.J. Blejer, and T.T. Wu, "Standing Waves and Notches in an EMP Simulator and Their Reduction," *IEEE Trans. Electromagn. Compatibil.*, EMC-23, 80-87, May 1981.

3. H.M. Shen and R.W.P. King, "The Rhombic EMP Simulator," *IEEE Trans. Electromagn. Compatibil.*, EMC-24, 255-265, May 1982.

4. H.M. Shen and R.W.P. King, "Experimental Investigation of the Rhombic EMP Simulator: Comparison with Theory and Parallel-Plate Simulator," *IEEE Trans. Electromagn. Compatibil.*, EMC-24, 349-355, August 1982.

5. H.M. Shen, R.W.P. King, and T.T. Wu, "An Experimental Investigation of the Rhombic EMP Simulator under Pulse Excitation," *IEEE Trans. Electromagn. Compatibil.*, EMC-25, 40-46, Feb. 1983.

6. H.M. Shen, R.W.P. King, and T.T. Wu, "Theoretical Analysis of the Rhombic Simulator under Pulse Excitation," *IEEE Trans. Electromagn. Compatibil.*, EMC-25, 47-55, Feb. 1983.

7. H.M. Shen, R.W.P. King, and T.T. Wu, "An Investigation of the Parallel-Plate EMP Simulator with Single-Pulse Excitation," *IEEE Trans. Electromagn. Compatibil.* (submitted for publication).

8. H.M. Shen, "The Time Domain Solution of the Current Integral Equation," *IEEE Trans. Antennas Propagat.* (submitted for publication).

III.5 Resource Allocation With Nonseparable Payoff. Y.C. Ho, Z.J. Yang, and L. Servi, Contracts N00014-75-C-0648 and NSF-ENG78-15231; Research Unit 9.

Continuing the research described in Section III.6 of the 1981-82 annual report, we extend the incentive-compatible allocation scheme to cases with non-separable group payoff. It is shown that the algorithm can be made converent and truth inducing under reasonable assumptions. A real world motivating example is included.

III.6 Inducible Regions of an Incentive Control Problem. T.S. Chang, Contracts N00014-75-C-0648 and NSF-ENG78-15231; Research Unit 9.

Using the inducible region approach, we study the closed-loop Stackelberg strategy for two-person multi-stage games. Necessary and sufficient conditions for the existence of such a strategy are derived by delineating the inducible region recursively. We also investigate some desirable properties for a leader's Stackelberg strategy. Along the optimal trajectory, if the leader has no incentive to deviate from his preannounced strategy even though he has a chance to change it, then the strategy satisfies the principle of optimality on the optimal trajectory. If the leader has no incentive to alter his pre-announced strategy when the follower deviates from the optimal trajectory, then the strategy fulfills the principle of optimality off the optimal trajectory. We discuss these two kinds of principle optimality and present the conditions for their existence. We demonstrate there always exists an optimal Stackelberg strategy among those leader's strategies which can induce the optimal strategy.

The inducible region approach is also extended to solve multifollower Stackelberg games, preliminary results show that the leader can induce a desired outcome in a dominant strategy environment.

III.7 Optimization and Control of Manufacturing Networks. R. Suri, Contracts N00014-75-C-0648 and ONR N00014-79-C-0776; Research Unit 9.

Following along the research direction stated in Annual Progress Report No. 94 (1980-81), we have developed new techniques for optimization of complex manufacturing networks. Two new methods, the phantom customer and marked customer networks, have been introduced as extensions of the perturbation analysis approach to discrete event systems. These methods enable efficient and accurate optimization of multiclass queueing networks with general service time distributions.[1] A use practical application of these methods is for otpimization of Flexible Manufacturing System (FMS) performance.

References

1. R. Suri and X. Cao, "The Phanton Customer and Marked Customer Methods for Optimization of Closed Queueing Networks with Blocking and General Service Times," submitted to ACM-SIGMETRICS Conference.

2. R. Suri and X. Cao, "Optimization of Flexible Manufacturing Systems Using New Techniques in Discrete Event Systems," Proc. 20th Allerton Conference on Communication Control and Computing, Monticello, Illinois, October 1982.

IV. ELECTROMAGNETIC PHENOMENA

Personnel

Prof. T.T. Wu
Prof. R.W.P. King
Dr. R. Bansal (summer)
Dr. J.T. deBettencourt
Dr. H.-M. Lee (until Aug. 31, 1982)
Mr. M.F. Brown
Mr. J.M. Dunn
Ms. M. Owens
Ms. B.H. Sandler
Mr. H.M. Shen

Research in the area of electromagnetic radiation is directed toward the solution of practical problems through the complete understanding of the underlying physical phenomena. This involves the coordinated application of modern analytical, numerical, and experimental techniques and the use of high-speed computers and precision instrumentation. Application is also made of modeling techniques and the principle of similitude. Most practically significant problems in this area are sufficiently complicated that extensive computation and measurement are often required to justify approximations that are usually necessary. Where possible, general formulas are obtained and verified experimentally so that the phenomenon under study can be understood physically in analytical form and not just as a set of numbers.

The researches are concerned primarily with the properties of antennas and arrays and of the electromagnetic fields they generate in various practically important environments that lead to difficult problems with complicated boundary conditions. Examples include dipoles, travelling-wave antennas and arrays, crossed dipoles, and loops near the boundary between two

media such as air and earth or sea water, and rock and sea water; dipoles in finite bodies composed of dielectric, conducting or layered materials; the currents in and fields between the conductors of a rhombic antenna; and the fields in the complicated geometry of electromagnetic pulse simulators with and without scattering obstacles.

IV.1 Theoretical and Experimental Study of the Scattering from an Obstacle Above the Earth. H.-M. Lee, T.T. Wu, and R.W.P. King, Contracts ARO DAAG29-79-C-0109 and N00014-75-C-0648; Research Unit 10.

The study of the electromagnetic field scattered from conducting objects on or near the surface of the earth has been completed.[1] This has been concerned primarily with the scattering from geometrically fat tubular cylinders. This choice of obstacle was made not only because an exact, free-space solution for the scattering from such a tubular cylinder was obtained during the course of this study, but also because this structure represents a 'composite' object which consists of a stack of wire loops. Thus, the scattering characteristics of a real target on or above the earth can be compared with those of fat cylinders of varying heights and diameters by means of a theoretical algorithm which makes use of our knowledge of the free-space solution and has been proved accurate by experimental check. A paper on the exact solution for the scattering current on a tubular cylinder in free space has been published.[2] The kernel of the integro-differential equations for the current excited on a tubular cylinder by an incident electromagnetic field is expanded in a complete set of orthogonal functions. The expansion coefficients are obtained explicitly as power series of the dimensions of the cylinder. As this kernel is a particular form of the

free-space Green's function, power-series representations for the Green's function in other forms are also presented to facilitate direct applications to other problems.

In a separate study, the currents in and the field scattered by a thin wire over a material half-space composed of earth, sea water, or lake water have been determined.[3] Full account is taken of the effect of the half-space on both the currents induced in the wire and on the scattered field. Distributions of current, back-scattering cross sections, and scattering patterns are given for both normal and non-normal incidence and with the incident field polarized in and perpendicular to the plane of incidence. The back-scattering cross section and the associated scattering patterns resemble those of the same wire when isolated but with greatly reduced amplitude. The data so far calculated show that the essential characteristics of the field scattered by a thin wire are preserved in the presence of a material half-space when the height d above the surface equals or exceeds about $d/\lambda_1 \sim 0.02$.

References

1. H.-M. Lee, "Electromagnetic Scattering of a Loop Above a Half-Space: Theory and Experiment," Ph.D. Thesis, Harvard University, Cambridge, MA, 1981.

2. H.-M. Lee, "Double Series Expansion of the Green's Function for a Perfectly Conducting Tubular Cylinder of Finite Length," *Radio Science*, vol. 18, 48-56, Jan.-Feb. 1983.

3. R.W.P. King and L.C. Shen, "Scattering by Wires near a Material Half-Space," *IEEE Trans. Antennas Propagat.*, vol. AP-30, 1165-1171, Nov. 1982.

IV.2 Theoretical and Experimental Study of the Field on the Surface of the Earth Scattered by a Buried Object. H.-M. Lee, T.T. Wu, and R.W.P. King, Contract Sandia-68-0404 and N00014-75-C-0648; Research Unit 10.

A scale model study of controlled source audio magneto-telluric (CSAMT) surveys is in progress. It is the logical continuation of the previous scattering problem in which the obstacle was above the water. The purpose is to study how well the boundaries of the objects can be defined by looking at the scattered fields.

A circular pool, four feet high and eighteen feet in diameter, has been installed in the basement of the McKay Laboratory. The pool was first filled with tap water to a depth of 116.5 cm; later a quantity of salt was added to the tank. A wooden frame was erected above the tank to support microwave absorbers, the transmitter, and the driving train of the probe set. A shielded probe is used to detect and measure the horizontal magnetic field. At its center is a short dipole which is used to measure the horizontal electric field. The cables are enclosed in a brass tube which is held vertically in a carriage that can tavel in a 50 cm by 50 cm square area in 1 cm steps. A motor is attached to the brass tube to rotate the probles through a 90° angle so that the two mutually perpendicular polarizations of the tangential electric and magnetic fields near the surface of the water can be measured. The center of the probes is located 2.8 cm above the water. This height can be adjusted.

A two-stage telescoping plastic column to hold the scattering object is located at the center of the water tank. The upper section can travel vertically for a total distance of 18 in. The lower sections holds the upper section to within a 0.4 cm deviation from the center. On top of the

column is a removable holder to which different objects can be attached. The telescoping section is chain-driven from outside the tank.

Preliminary measurements were taken at an operating frequency of 300 MHz of the field scattered by a metal disc in tap water and in salt water. The data are very promising. The modification of previously available computer programs for the scattered fields of a loop near a two medium interface to accommodate complex wave number is underway. This program will be helpful in interpreting experimental data.

IV.3 Numerical and Analytical Determination of Fields of Antennas Near an Interface Between Two Half-Spaces with Significantly Different Wave Numbers. T.T. Wu, R.W.P. King, and B.H. Sandler, Contracts N00014-75-C-0648 and N00014-79-C-0419; Research Unit 10.

Until recently the theoretical tools available for the study of the propagation of electromagnetic waves in a region composed of two half-spaces filled with two different material media included: 1) the general complex integrals originally due to Sommerfeld for the field of an infinitesimal dipole parallel or perpendicular to the plane boundary, and 2) simple approximate formulas due to Baños for the field in restricted, nonoverlapping ranges of the parameters. At Harvard a detailed numerical evaluation of the general integrals for the radial electric field due to a horizontal electric dipole in a half-space of earth or water bounded by air has been carried out and compared with Baños' approximate formulas.[1,2] For a complete physical understanding of the direct and lateral-wave components of the electromagnetic field, their interaction and reflection and transmission at boundaries, the general integrals are too involved

and the approximate formulas neither very accurate nor very useful since they have different forms in disconnected ranges. In order to overcome these difficulties, the general integrals have been evaluated directly, subject to conditions that are easily satisfied, and simple accurate formulas have been obtained that are valid over the entire practical range. The newly drived formulas for the electric field due to a horizontal electric dipole have already been reported.[3,4] Similar formulas for the remaining magnetic-field components of the horizontal dipole and for the complete electromagnetic field of a vertical electric dipole are now available.[5,6] The formulas involve only simple exponential functions and error functions and their accuracy has been checked in detail against numerical calculations from the general integrals.

The significance of these new formulas is considerable. Simple inspection revealed that there must be an interference pattern in the amplitudes and phases of the components due to the interaction of the clearly separated lateral and direct waves. Detailed computations have for the first time demonstrated the existence of such patterns in all media.[3] Recomputation from the general integrals with greatly reduced intervals of distance has shown very close agreement with the approximate formulas. The time required for the data from the new formulas is measured in fractions of a minute, that from the general integrals in many hours. The new, accurate and simple formulas open a hitherto closed door to the quantitative study of lateral waves and the physical understanding of their properties.

References

1. R.W.P. King, B.H. Sandler, and L.C. Shen, "A Comprehensive Study of Subsurface Propagation from Horizontal Electric Dipoles," *IEEE Trans. Geosci. and Remote Sensing*, vol. GE-18, 225-233, July 1980.

2. R.W.P. King, G.S. Smith, M. Owens, and T.T. Wu, *Antennas in Matter*, Ch. 11, The M.I.T. Press, Cambridge, MA, 1981.

3. T.T. Wu and R.W.P. King, "Lateral Waves: A New Formula and Interference Patterns," *Radio Science*, vol. 17, 521-531, May-June 1982.

4. T.T. Wu and R.W.P. King, "Lateral Waves: New Formulas for $E_{1\phi}$ and E_{1z}," *Radio Science*, vol. 17, 532-538, May-June 1982.

5. R.W.P. King and T.T. Wu, "Lateral Waves: Formulas for the Magnetic Field," *Journal of Applied Physics*, vol. 54, 507-514, Feb. 1983.

6. R.W.P. King, "New Formulas for the Electromagnetic Field of a Vertical Electric Dipole in a Dielectric or Conducting Half-Space Near its Horizontal Interface," *Journal of Applied Physics*, vol. 53, 8476-8482, Dec. 1982.

IV.4 Reflection and Scattering of Lateral Waves at Vertical Discontinuities.

R.W.P. King, Contracts N00014-75-C-0648 and N00014-79-C-0419; Research Unit 10.

Electromagnetic waves are useful in geophysical exploration and remote sensing primarily when the properties of electromagnetic propagation are completely understood in terms of the characteristics of the media through or along which they are transmitted. Some of the most interesting aspects of the earth are related to regions near the boundaries of quite different materials. In some instances the regions along the bounding surfaces are relatively smooth, in others they are interrupted by discontinuities, projections and depressions. The propagation of electromagnetic waves along boundaries between quite different media is predominantly by lateral waves. This is well understood along smooth boundaries, but the scattering of lateral waves at boundaries and discontinuities is not well understood.

A study has been made[1] of the effect on the field generated by a horizontal dipole due to vertical discontinuities on both sides of the boundary between earth (water) and air. The two types of reflecting boundaries considered consist of: a) vertical discontinuities in the denser medium (earth, water) in the form of changes in the wave number from k_1 to k_3; and b) vertical projections into the less dense medium (air) in the form of thin walls of the denser medium. The analysis shows that reflections from the discontinuities in the denser half-space are extremely small even when k_1 changes from a value characteristic of salt water to a value $(k_3 \to \infty)$ characteristic of a perfect conductor (metal). Reflections from metal walls in air when $k_3 \sim \infty$ are much larger but still quite small when the height of the wall is a tenth of a wavelength or less. They are very significant when the wall is a quarter-wavelength high. These results are readily understood if it is recalled that the vertical unit dipole in air is very superior to the vertical unit dipole in salt water as a generator of lateral waves. Standing-wave patterns due to incident and reflected lateral waves are determined and shown graphically. An experimental study to measure reflections of lateral waves at discontinuities and boundaries is discussed under the next heading.

Reference

1. R.W.P. King, "On the Reflection of Lateral and Waves from Perpendicular Boundaries," *IEEE Trans. Geosci. and Remote Sensing* (submitted for publication.

IV.5 Lateral-Wave Propagation and Modeling of the Lithosphere. M.F. Brown, R.W.P. King, T.T. Wu, and J.T. deBettencourt, Contracts N00014-79-C-0419 and N00014-75-C-0648; Research Unit 10.

Experimental work was originally carried out at $f = 600$ MHz in a rectangular tank $(12' \times 8' \times 1')$ containing salt water. The extensive measurements showing the rate of decay of lateral waves in agreement with theory, the surprisingly small effect of obstacles and depressions on the propagation, and the scattering from metal cylinders have been reported.[1] These measurements were complicated by reflections from the side walls. To reduce side-wall reflections, a directional array of two traveling-wave antennas was developed as the source and movable metallic sheets were placed along the sides of the tank.

In order to eliminate all reflections from side walls, the tank was rebuilt in a semicircular geometry (6' radius) which permits only normally incident reflections of outgoing cylindrical waves from the circular boundary; there are no side walls. The modified tank consists of two sections, the main semicircular part with radius ρ_b and a peripheral region just outside the semicircle $(\rho > \rho_b)$ which can be left empty or filled with water or other material for studying reflections from and absorption at the cylindrical boundary.

Extensive measurements have been completed in the semicircular tank on the transmission and reflection of lateral waves. A new verification was made of the theoretical $1/\rho$ rate of decay with distance of $E_{1\rho}$ in the intermediate zone in the absence of side-wall reflections. The fields incident upon and scattered from the various obstacles tested in the rectangular tank agree well with comparable ones in the new tank. Thus, the scattering effects reported earlier[1] are of general validity, and not peculiar to the fields in a tank bounded on the sides by metallic surfaces.

The reflections of lateral waves at cylindrical discontinuities above and below the salt-water surface have been measured[2,3] in the semicircular model lithosphere at two frequencies, f = 644 MHz and f = 1.5 GHz. Simple combinations of horizontal and vertical metal planes were chosen as the discontinuities. The measurements confirmed the theoretical predictions (discussed under the previous heading). The small reflections from the ceiling were also studied experimentally and theoretically in their effect on both traveling and standing lateral waves. The measured $E_{1\rho}$ field patterns involve, in general, three waves: 1) The direct lateral waves with both vertical and radial components traveling radially outward from the source; 2) reflections from the cylindrical boundary in the form of lateral waves traveling radially inward toward the source and producing a regular standing-wave pattern; and 3) transverse plane waves coming from the ceiling at normal or near normal incidence and polarized with the electric field in the radial direction. These produce interference patterns with traveling and standing lateral waves that are quite different from ordinary standing waves produced by similar waves traveling in opposite directions. It appears that the complications introduced by the finite size and indoor location of the tank are now well understood.

References

1. M.F. Brown, R.W.P. King, and T.T. Wu, "Lateral-Wave Studies in a Model Lithosphere," *Journal of Applied Physics*, vol. 53, 3387-3396, May 1982.

2. M.F. Brown, R.W.P. King, and T.T. Wu, "Experiments on the Reflection of Lateral Waves," *IEEE Trans. Geosci. and Remote Sensing* (submitted for publication).

3. M.F. Brown, R.W.P. King, and T.T. Wu, "The Propagation and Reflection of Lateral Waves," (accepted for presentation at the International IEEE/AP-S Symposium at Houston in May 1983).

IV.6 Theoretical and Experimental Studies of Lateral-Wave Propagation.
J.M. Dunn, Contract N00014-75-C-0648; Research Unit 10.

Currently there is interest in the possibility of investigation by electromagnetic means the electrical properties of the earth beneath the ocean floor. For this a knowledge is required of the nature of wave propagation in layered media (e.g., a layer of sediment over rock, or a layer of rock over a highly conducting mantle). A study is now in progress of the field due to a horizontal dipole located near a salt-water/air interface with a perfectly conducting top plate placed above the air region. The salt water represents the ocean, the air region is the analog of a rock layer, and the top plate corresponds to the highly conducting mantle. The exact integral solution has been evaluated numerically for the radial electric field in the sea water.[1] It is found that the insertion of the top plate changes the field patterns from those characteristic of the simpler case of two half-spaces (see heading #3). When the top plate is added at a height L that is less than 0.5 air wavelengths, there is an exponential decay in the field patterns. For $L >$ [illegible], oscillations start to appear, superimposed on top of this decay. As L is increased, more and more oscillations contribute to produce increasingly more complicated field patterns. Work is nearing completion on an analytical approximation that will explain these oscillations. Future work is planned for three layers consisting of sea water, sediment, and rock.

An experimental study to test lateral-wave antenna arrays has been initiated, new items of equipment have been purchased, and the major part of the system's construction has been completed. The purpose of this study is to determine how to transmit lateral-wave-type signals effectively. Transmitting antennas will be placed in the center of a circular tank, just

below the water surface. The lateral-wave field will then be measured by a receiving antenna located at various distances from the transmitter. Subsequently, it may be possible to investigate the three-layer problem (with top plate), using the same experimental setup.

Reference

1. J.M. Dunn, "Effect of Perfectly Conducting Top Plate on Lateral-Wave Propagation," (accepted for presentation at the International IEEE/AP-S Symposium at Houston in May 1983).

IV.7 The Wave Antenna for Transmission and Reception.

R.W.P. King,
Contract N00014-75-C-0648; Research Unit 10.

An important directional antenna for transmission (communication, radar) between points on or near the surface of the earth is the wave antenna known as the Beverage antenna. It consists of a long wire parallel and close to the surface of the earth (sea, lake, ice). It is driven and terminated in a manner to provide a traveling wave of current. The Beverage antenna has been discussed by numerous authors primarily as a directional receiving antenna. The usual approach is to represent the ground as a complex dielectric and consider the total pattern of the antenna and its properly weighted image. This approach disregards the effect of the earth on the distribution of current in the horizontal wire and assumes that a valid image can be constructed to replace the earth. Furthermore, it fails to provide a means for determining the field along the surface of the earth where a lateral wave dominates.

The current in and driving-point admittance of a horizontal-wire antenna over the earth have been determined for antennas terminated to carry currents with both standing- and traveling-wave distributions.[1] It has been shown that when the horizontal wire is close to the earth, the wave number characteristic of the distribution of current is significantly different from the free-space wave number. The adjacent conducting or dielectric half-space has a dominant effect on the current in the conductor and cannot be disregarded any more than can the sheath of a coaxial line. In effect, the horizontal wire is an eccentrically insulated conductor lying on the surface of the material half-space (Region 1), where the thickness of the air insulation is essentially the height d of the wire.

Of primary interest in the applications of the wave antenna is the field along the surface of the earth. No accurate determination of this field appears to be available in the literature. An analysis has now been completed[2] of the traveling-wave horizontal-wire antenna over the earth in its original form with vertical ground connections (Beverage antenna) and with these replaced by horizontal terminations. The transmitting and receiving qualities of the antennas have been determined specifically for transmission and reception of waves traveling along the surface of the earth. Full account is taken of the effect of the earth on the currents in the antenna and its terminations. For transmission, the electromagnetic field of an antenna with optimum length is determined, using the newly derived approximate expressions for the electromagnetic field in Region 1 and on the boundary in Region 2 (air) due to horizontal and vertical dipoles (see heading IV.3). The relative contributions to the field from the main horizontal wire and the vertical or horizontal terminations have been determined. For reception, the induced currents in the antenna and in the load are derived for a field incident along the surface of the earth.

References

1. R.W.P. King, G.S. Smith, M. Owens, and T.T. Wu, *Antennas in Matter*, pp. 89-109, The M.I.T. Press, Cambridge, MA, 1981.

2. R.W.P. King, "The Wave Antenna for Transmission and Reception," *IEEE Trans. Antennas Propagat.* (submitted for publication).

IV.8 Theoretical and Experimental Study of a Loop Antenna with Cylindrical Core. R.W.P. King, R.W. Burton, and T.T. Wu, Contract N00014-75-C-0648 and Southeastern Center for Electrical Engineering Education, Inc.; Research Unit 10.

The problem of long-range communication over or into the earth or the sea has been investigated on numerous fronts. These include the Sanguine-Seafarer project with an extensive antenna buried in the earth over a layer of low-loss rock; waveguide-like transmission in such a layer of rock; lateral-wave propagation along the air-earth, air-ocean, or ocean-lithosphere boundary, etc. The possibility of low-frequency radiation from a physically large, but electrically small loop constructed with conductors extending down on two sides of a mountain, possibly on an island in the ocean, with the lower ends grounded or joined by a third conductor in a tunnel through the mountain has been suggested. A theoretical and experimental study of the electromagnetic field of an electrically small loop antenna around a cylindrical core of arbitrary material has been completed.[1] The analytically derived field of a loop around an infinitely long circular, conducting or dielectric cylinder is compared with measurements made on half of such a structure over a ground plane. With the help of the principle of similitude, measurements made with a small loop at a high frequency with cylinders of water with widely different conductivities are applied to a very large loop

around a mountain at a very low frequency. The measurements carried out at a high frequency using an electrically small loop indicate that at least for the field in the plane of the loop the cyclinder of matter can be approximated by an image loop with an empirically evaluated current.

Reference

1. R.W. Burton, R.W.P. King, and T.T. Wu, "The Loop Antenna with a Cylindrical Core: Theory and Experiment," *IEEE Trans. Antennas Propagat.*, vol. AP-31, 225-231, March 1983.

IV.9 Subsurface Communication or Heating with Embedded Insulated Antennas.

R.W.P. King, Contract N00014-75-C-0648, with S. Prasad of Northeastern University and with B.S. Trembley and J.W. Strohbehn of Dartmouth College; Research Unit 10.

When an antenna is to be used in a material medium like the earth or a living organism either for purposes of communication and telemetry or for local heating, its configuration is often constrained by the need to insert it with its feeding transmission line into a hole that is very deep compared to its cross-sectional dimension. Usually the antenna and its transmission line must be insulated from the surrounding earth or flesh. A theoretical and experimental study has been completed[1,2] of the properties of insulated antennas embedded at a considerable depth below the surface of a living organism or of the earth. Special attention has been given to devising methods of transmitting power for localized radiation or heating. Four different insulated coaxial lines and antennas with interesting and useful properties when inserted in a hole in a general dissipative medium have been studied. The analysis, based on the theory of the insulated antenna, shows that the insulated conductor embedded in an electrically dense, conducting

or dielectric medium is a versatile device for communication or heating in the earth or a living organism. It can be operated as a resonant element or as a traveling-wave antenna and, with appropriate dimensions, is useful at frequencies ranging from the highest to moderately low. Although the theory of the center-driven insulated antenna has been confirmed experimentally, its application to the several practical structures under study involves a number of approximations which require experimental validation. An experimental study of the different insulated antenna-transmission-line structures was carried out[2] and the results show that the theory of the insulated antenna may be used with accuracy to predict the behavior of insulated antennas with complicated structures.

One application of insulated antennas used for localized heating is the insertion of an insulated antenna into a tumor to produce local hyperthermia in conjunction with radiation therapy. This application requires antennas of very small size operated at a very high frequency. A theoretically similar but practically very different use of insulated antennas for localized heating is in the extraction of shale oil. For this purpose very large insulated antennas are inserted into boreholes in the shale and heated at an appropriate much lower frequency. In both applications interest is primarily in the field quite close to the antenna where most of the heating takes place. The *near* electric field of a bare or insulated dipole in a medium like muscle or earth is much more involved than the far field because it is elliptically polarized. Simple expressions in closed form are not available. The determination of the field of an insulated dipole is further complicated by the fact that the wave number of the current in the antenna is complex and different from the wave number of the surrounding medium. A theoretical study of this subject has been completed.[3] The distribution of

current in and the admittance of a center-driven dipole embedded in a general medium are reviewed. Formulas for the electric field generated by the currents in the dipole are derived for all points outside the antenna. Formulas for the polarization ellipses of the field near the antenna are derived and evaluated for antennas with electrical half-lengths $\beta_L h = \pi/4$, $\pi/2$, π, and $3\pi/2$.

References

1. R.W.P. King, L.C. Shen, and T.T. Wu, "Embedded Insulated Antennas for Communicating and Heating," *Electromagnetics*, vol. 1, 51-72, April 1981.

2. S. Prasad and R.W.P. King, "Experimental Study of Embedded Insulated Antennas," *IEEE Trans. Antennas Propagat.*, vol. AP-30, 1013-1017, Sept. 1982.

3. R.W.P. King, B.S. Trembly, and J.W. Strohbehn, "The Electromagnetic Field of an Insulated Antenna in a Conducting or Dielectric Medium," *IEEE Trans. Microwave Theory and Techniques* (submitted for publication).

IV.10 Theoretical and Experimental Study of Electromagnetic Fields and Antennas in Dissipative and Dielectric Cylinders. R. Bansal, Contract N00014-75-C-0648; Research Unit 10.

The investigation of the induced electromagnetic fields inside a finite dielectric cylinder illuminated by a plane wave has been completed.[1-3] The theoretical solution for the finite dielectric cylinder proceeds in two steps. By taking advantage of the fact that water has a large (in general, complex) relative dielectric constant, it has been possible to "decouple" the internal absorption problem from the external scattering problem. First the external problem is solved numerically using a surface integral-equation solution and the tangential magnetic field $\vec{H}_{tan}$ on the surface of the

cylinder is computed. This $\vec{H}_{tan}$ then serves as the boundary condition for an analytical eigenfunction solution of the internal problem. Since the internal problem is solved analytically, it is possible to incorporate into the theoretical model the central conducting tube of the experiment without significantly increasing computation time or labor. (The conducting tube was required in the experimental setup to shield the transmission lines leading to the probes.) The basic procedure can be iterated for improved accuracy. The computer implementation of the method is very economical since only a single integral equation needs to be solved numerically. The iterative scheme used in the method shows rapid convergence for dielectrics characterized by a large real permittivity *and* a moderately high loss tangent; hence, the method is particularly suitable for biological applications. The iterative scheme is only partially successful, at best, when applied to a dielectric cylinder possessing a large real permittivity but a small conductivity (e.g., distilled water). This breakdown of the iterative scheme is believed to be closely related to the internal "resonances" of the dielectric cylinder. A comparison of sample calculations for salt-water cylinders and corresponding experimental results shows good agreement. The experimental measurements were carried out at 100, 300 and 600 MHz. The conductivity of the 50-cm-long column of water was varied from approximately zero to 3.5 S/m.

References

1. R. Bansal, "A Theoretical and Experimental Study of Electromagnetic Fields in Finite Dielectric Cylinders," Ph.D. Thesis, Harvard University, Cambridge, MA, 1981.

2. R. Bansal, T.T. Wu, and R.W.P. King, "Analysis of Finite Dielectric Bodies in a Plane-Wave Field," *IEE Proc.*, vol. 129, Part H, 116-122, June 1982.

3. R. Bansal, R.W.P. King, and T.T. Wu, "The Measurement of the Electric Field inside a Finite Dielectric Cylinder Illuminated by a Plane Wave," *IEEE Trans. Microwave Theory and Techniques*, vol. MTT-30, 1282-1286, Aug. 1982.

IV.11 Theoretical and Experimental Study of the Rhombic Antenna as an EMP Simulator under CW Excitation. H.M. Shen and R.W.P. King, Contracts N00014-75-C-0648 and F29601-81-K-0010 (Experiment only); Research Unit 10.

In order to obtain greater insight into the physical phenomena associated with a transmission-line type EMP simulator (see heading #12), it has seemed desirable to make use of a structure that permits an accurate analytical determination of the currents in the conductors and of the electromagnetic fields they generate, while still approximating the actual simulators in general shape. Such a structure consists simply of the two-conductor rhombic antenna. It is well known that this type of rhombic antenna has broad-band properties. However, early analyses have been concerned exclusively with the far field and not with an accurate determination of the currents in the conductors and especially of the field between them which is of interest in its possible application as an EMP simulator. Note that in the rhombic simulator the currents at all frequencies are confined to electrically thin conductors that, in effect, are located along the edges of the metal-plate or wire-mesh simulators where the largest current density is to be found.

A complete analysis has been made of the two-conductor rhombic antenna as an EMP simulator.[1] The distributions of current along the conductors and the electric field in the working space bounded by them have been determined. They are very well approximated by quite simple, zero-order formulas.

When the structure is terminated in the characteristic impedance, the currents are very nearly traveling waves and this is true over a wide frequency band. At low frequencies when the distance between the conductors is everywhere electrically small, the structure behaves like a simple transmission line. As the frequency is raised to intermediate and high values with the wires several wavelengths apart at the center of the simulator, the traveling-wave nature of the current and the associated electric field is still quite well maintained. The terminating impedance continues to be effective at the high frequency even though a significant fraction of the power supplied by the generator is radiated. The electric field in the working space bounded by the conductors exhibits a reasonably constant amplitude with a low standing-wave ratio of 1.5 at all frequencies.

The rhombic simulator has also been investigated experimentally.[2] The results have been compared at low, intermediate and high frequencies with both the theory and earlier measurements made on the Harvard model simulator with its central parallel-plate section and tapered metal-plate feeding and loading ends. The agreement with theory is very good. Similarities and differences are observed between the fields in the working volumes of the rhombic-wire and the metal-plate simulators. In general, the rhombic-wire simulator provides a field more nearly like that of a traveling transverse wave in unbounded space. The rhombic simulator has the advantage that a complete and accurate theory is available, which is not the case of the metal-plate simulator.

References

1. H.M. Shen and R.W.P. King, "The Rhombic EMP Simulator," *IEEE Trans. Electromagn. Compatibil.*, vol. EMC-24, 255-265, May 1982.

V. SIGNIFICANT ACCOMPLISHMENT REPORT

V.1 Submillimeter-Wave Properties of Small-Area Tunnel Junctions. W.C. Danchi, F. Habbal, and M. Tinkham, Contract N00014-75-C-0648; Research Unit 2, SOLID STATE ELECTRONICS.

The ac Josephson effect and the photon-assisted tunneling effect in superconducting tunnel junctions have received a great deal of attention because of their promise for use in high-performance detectors and mixers of millimeter and submillimeter wave radiation. The former effect is based on the superconducting electrons, while the latter is based on nonlinearities in ordinary quasiparticle tunneling resulting from the superconducting energy gap. High junction capacitance has heretofore limited their use to the millimeter and longer wavelength region of the spectrum. In the earlier work, only point contacts[1] have had low enough capacitance to function in the far-infrared or submillimeter region. Here we report the first observations of both these effects at submillimeter wavelengths using small-area photolithographically fabricated thin-film superconducting tunnel junctions, rather than point contacts.

Our Sn-SnO-Pb junctions were fabricated at the center of resonant half-wave antenna structures, to facilitate coupling to the incident radiation, which was produced by a home-made optically-pumped FIR laser. Most of our data were taken using the strong CH_3F line at 604 GHz ($\lambda = 496$ μm), but we have also made similar measurements with the 246 GHz ($\lambda = 1.22$ mm) laser line. The junctions used had resistances ranging from 16 to 380 ohms.

Considering first the ac Josephson effect, at 604 GHz, a 176 ohm junction with area $\sim 5 \times 10^{-9}$ cm^2 showed up to 7 Josephson steps (~ 8 mV), a performance

comparable with that observed earlier in point contacts. The variation of the steps widths with laser power was found[2] to agree well with theoretical predictions. We observed a marked variation of step shape with the junction resistance. Low resistance, large-area junctions ($R \sim 20$ ohms, $A \sim 2.5 \times 10^{-8}$ cm^2) had Josephson steps that were flat and well fitted by the RSJ model prediction for the step shape, but these junctions did not couple efficiently to the radiation due to the severe impedance mismatch between junction and antenna (largely caused by capacitive shunting). The high resistance, smaller-area junctions ($R \sim 170$ ohms, $A \sim 5 \times 10^{-9}$ cm^2) coupled well to the radiation, but the Josephson steps were not flat, and they were also substantially rounded by noise. This rounded and tilted step shape was found[3] to be fitted reasonably well by using the simplified theory of P.A. Lee[4] with a noise temperature of 10-20 K and an appropriate estimate of the junction capacitance. However, we are now developing a more comprehensive analysis of noise effects using computer simulations. In these simulations, we use a modified RSJ model which takes account of the full nonlinearity of the quasiparticle I-V curve, and uses it with the theory of Rogovin and Scalapino[5] to determine a power spectrum that includes shot noise effects and zero-point fluctuations in addition to conventional Johnson noise. Our preliminary results indicate that the shot noise accounts for the rounding of the high-voltage steps without recourse to an elevated temperature, and that the large suppression of the zero-voltage critical current can also be explained naturally with this more accurate frequency-dependent power spectrum. This computer analysis is now moving ahead quite rapidly, and further results should be available in the near future.

Turning now to the photon-assisted tunneling features, these provided a very comprehensive test of the Tien-Gordon[6] theory, which predicts that I-V curves in the presence of radiation can be computed from those in the absence

of radiation in a simple way. Our results[7] show that this theory gives an excellent account of the shape of the photon-assisted tunneling features and of their dependence on laser power. The cleanest test of the theory was made at 4.2 K, above T_c(Sn), where the junctions are S-I-N devices in which the complications of the Josephson effect are absent. By plotting the change in dc current at a particular dc bias voltage as a function of the laser power, and finding its slope in the low-power limit, we were able to infer the responsivity R. When biased at the gap voltage, we measured a responsivity consistent with the value 0.47 $(e/h\omega)$ computed using the Tien-Gordon theory. This result implies performance within a factor of two of the quantum limit $(e/h\omega)$, which corresponds to transfer of one electron across the barrier for each photon absorbed.

In addition to the noise modeling mentioned above, further experimental work is underway to investigate the frequency dependence of various antenna coupling schemes, and to explore the roll-off of the ac Josephson effect at frequencies above the energy gap.

References

1. D.A. Weitz, W.J. Skocpol, and M. Tinkham, *Appl. Phys. Lett.* 31, 227 (1977).
2. W.C. Danchi, F. Habbal, and M. Tinkham, *Appl. Phys. Lett.* 41, 883 (1982).
3. W.C. Danchi, F. Habbal, and M. Tinkham, *IEEE Trans. Mag.*, in press.
4. P.A. Lee, *J. Appl. Phys.* 42, 325 (1971).
5. D. Rogovin and D.J. Scalapino, *Annals of Physics* 86, 1 (1974).
6. P.K. Tien and J.P. Gordon, *Phys. Rev.* 129, 647 (1963).
7. F. Habbal, W.C. Danchi, and M. Tinkham, *Appl. Phys. Lett.* 42, 296 (1983).

V.2 Nonequilibrium Switching Phenomena on Picosecond Time Scales. D.J. Frank and M. Tinkham, Contract N00014-75-C-0648; Research Unit 2, SOLID STATE ELECTRONICS.

When a superconducting filament is subjected to an applied current step in excess of the critical current, transient phenomena occur of intrinsic time scales typically of order $10^{-8} - 10^{-12}$ seconds, after which the filament becomes fully resistive. The characteristic time scale is long in weak-coupled (low T_c) superconductors such as Al, and short in stronger-coupled ones such as Pb or In, but it also depends on the level of supercritically of the current level, on the temperature, and on the specific phenomenon observed. We have been carrying on a program of measuring these responses, both with conventional room-temperature fast electronics and with the Faris[1] picosecond sampler based on the IBM Josephson computer technology, together with extensive theoretical modeling of the nonequilibrium electronic phenomena in the filament. This work to date has been recorded in the recent Ph.D. thesis[2] of D.J. Frank.

Among the highlights of our experimental results using the cryogenic picosecond sampler is the first observation of the "inductive" voltage spike when the current step is first applied. This voltage pulse (of height $\sim$100 μV and duration $\sim$50 psec) is needed primarily to accelerate the supercurrent (i.e., the "kinetic" inductance exceeds the geometric inductance in these fine filaments); after this pulse, the voltage drops to a much lower value as the current is carried as supercurrent. This reduced voltage is zero if $I < I_c$, and it is non-zero if $I > I_c$, since in the latter case there is need for a slight continuing acceleration of the supercurrent velocity as the *number* of superconducting electrons is falling in response to the pair-breaking effect of the current. Finally, the Cooper pair density falls

Two-photon transitions have been observed for Gd^{3+} in aqueous solution. Fine structure splittings, similar to crystal field splittings, have been observed which indicate a low symmetry quasi-static environment. The two-photon transition $^8S_{7/2} \rightarrow {}^6P_{7/2}$ has been detected in Eu^{2+}: BaF_2, although surprisingly relaxation occurs via energy transfer to neighboring Eu^{3+} impurity ions, which fluoresce in the red. These observations are being further investigated.

References

1. M.C. Downer, "Two-Photon Spectroscopy of Rare Earth Ions in Condensed Matter Environments," Ph.D. Thesis, Harvard University, February 1983.

2. M.C. Downer, A. Bivas, and N. Bloembergen, "Selection Rule Violation, Anisotropy, and Anomalous Intensity of Two-Photon Absorption Lines in Gd^{3+}: LaF_3," *Opt. Comm.* 41, 335 (1982).

3. M.C. Downer, A. Bivas, and N. Bloembergen, "New Third-Order Contributions to Two-Photon Absorption Line Strengths in Gd^{3+}: LaF_3," *Appl. Phys.* B28, 281 (1982).

II.3 Laser-Induced Ordering in Matter. N.W. Carlson, A.G. Yodh, and T.W. Mossberg, Contract N00014-75-C-0648 and NSF Grant THY-82-07080; Research Unit 5.

The initial experimental apparatus for the study of laser-induced ordering in gases was completed and preliminary experiments were performed. We have developed a new approach to generating photon echoes in gases which demonstrates the interplay between coherent transients and phase conjugation. We found that any echo excitation scheme which is modified by the addition of a final standing-wave pulse, will generate a backward-propagating phase-conjugate "replica"--termed standing-wave-induced backward echo[1,2] of the normal photon echo. The normal echo--generated without the standing wave--

and the backward echo have comparable magnitude and occur simultaneously; however, the backward echo is much easier to detect since it propagates antiparallel to the normal echo. The ease with which the backward echo can be detected makes this new approach very attractive for the study of gas phase relaxation processes.

We have produced standing-wave-induced backward two-pulse photon echoes on the $2\,^2S - 2\,^2P$, 671 nm transition of lithium. A strong decrease in the backward echo intensity was observed when the standing wave was oriented at large angles from the normal excitation pulses. This may be due to the phase randomness across the spectral profile of the non-Fourier-transform excitation pulses from the dye laser. At large standing-wave angles, an ensemble of randomly phased spectral components of the standing-wave pulse contribute to producing the backward echo thus reducing the net backward echo polarization. The effect of excitation pulse incoherence on echo intensity has never before been observed or studied.

Further experiments with standing-wave-induced photon echoes are planned, including a demonstration of the phase conjugate nature of the backward echo and studies of collisional processes in gases using backward echoes.

Experiments to study laser-induced ordering in condensed matter are also planned. The construction of laboratory equipment for these experiments is underway.

References

1. N.W. Carlson, A.G. Yodh, and T.W. Mossberg, "Standing-Wave-Induced Backward Photon Echoes," (submitted to *Phys. Rev. Lett.*).

2. N.W. Carlson, A.G. Yodh, and T.W. Mossberg, "Standing-Wave-Induced Backward Photon Echoes," submitted as a contributed paper to the Fifth Rochester Conference on Coherence and Quantum Optics.

II.4 Picosecond Laser Interactions with Semiconductors. J.M. Liu, L.A. Lompre, H. Kurz, and N. Bloembergen, Contracts N00014-75-C-0648 and ONR 00014-83-K-0030; Research Unit 6.

The picosecond time-resolved transmission and reflectivity measurements, announced in the preceding Annual Progress Report No. 95, have been carried out on thin crystalline silicon films on sapphire. In the first series of experiments the picosecond pump pulse was at the second harmonic of the Nd-YAG laser ($\lambda = 533$ nm), the probe pulse with a much smaller diameter to monitor only the central portion of the heated silicon spot was at $\lambda = 1.06$ μm.

At pump energy fluences below the threshold for phase transitions, a modification of the complex index of refraction is observed due to the creation of an electron hole plasma. Above threshold a phase transition is induced on a picosecond time scale. The optical properties change to those characteristics for metallic liquid silicon. A brief communication has been published[1] and detailed descriptions of the experimental technique may be found in a doctoral thesis.[2] Results have also been published at several international meetings, since the subject of laser interactions with silicon is still under very active discussion.[3-6]

In the second half of this annual reporting period the probing wavelength has been changed to the visible wavelength ($\lambda = 533$ nm), while the pump wavelength is either the same or in the ultraviolet ($\lambda = 262$ nm). The thickness of the SOS samples has also been varied systematically. The new results for the index variations at $\lambda = 533$ nm enable us to deduce the temperature rise of the silicon below the threshold of the phase transformation.

Lattice temperatures of up to 1100°K have been deduced at 0.12 Joule/cm^2 which extrapolate nicely to the melt temperature of the surface at the threshold of 0.2 Joule/cm for phase transformation.

We plan to extend the probe wavelength to the near infrared. The index of refraction is here more sensitive to the kinetics of the electron-hole plasma.

References

1. J.M. Liu, H. Kurz, and N. Bloembergen, "Picosecond Time Resolved Plasma and Temperature Induced Changes of Reflectivity and Transmission in Silicon," *Appl. Phys. Lett.* 41, 643 (1982).

2. J.M. Liu, "Thermal Model of Picosecond Laser Interactions with Silicon," Ph.D. Thesis, Harvard University, unpublished 1982.

3. J.M. Liu, H. Kurz, and N. Bloembergen, "Picosecond Time Resolved Detection of Plasma Formation and Phase Transition in Silicon," in *Picosecond Phenomena III*, Garmisch-Partenkirchen, June 16-18, 1982, eds. by K.B. Eisenthal, R.G. Hochstrasser, H. Kaiser, and A. Lauberau.

4. H. Kurz, J.M. Liu, and N. Bloembergen, "Pulsed Laser Annealing of Semiconductors; Experimental Facts and Open Questions," *16th International Conference on the Physics of Semiconductors*, Montpelier, September 6-10, 1982.

5. J.M. Liu, H. Kurz, and N. Bloembergen, "Picosecond Time Resolved Detection of Plasma Formation and Phase Transition in Silicon," Materials Research Council Conference, Boston, November 1982, Proceedings to be published.

6. H. Kurz, J.M. Liu, and N. Bloembergen, "Ultrafast Phase Transitions in Silicon Induced by Picosecond Laser," ASI-Seminar CORSICA, *Coherent Properties of Semiconductors under Laser Irradiation*, ed. by L.D. Laude (Martinus Nijhoff, The Hague, 1983), in press.

7. L.A. Lompre, J.M. Liu, H. Kurz, and N. Bloembergen, "Time Resolved Temperature Measurements of Picosecond Laser Irradiated Silicon," submitted for publication in *App. Phys. Lett.*

II.5 Picosecond Laser-Induced Emission from Metals and Semiconductors.
J.M. Liu, L.A. Lompre, M. Malvezzi, H. Kurz, and N. Bloembergen,
Contracts N00014-75-C-0648 and ONR N00014-83-K-0030; Research Unit 6.

Although in the preceding Annual Progress Report it was announced that this project was to be terminated, this decision has been reversed in view of the continuing interest in the question of energy transfer between the laser-generated plasma and the lattice.

A series of experiments on charged particle emission from zirconium was performed with femtosecond pulses in a collaborative effort with the group of Professor E. Ippen at the Massachusetts Institute of Technology. The experimental apparatus available at M.I.T. consists of a mode-locked dye laser in a colliding pulse configuration. The 90 femtosecond pulse near $\lambda = 600$ nm are amplified by four dye laser amplifiers. The measured photoelectric emission data are significantly different from those obtained by us in the preceding year with 2 ps pulses. The electron emission saturates before the onset of positive ion emission. The interpretation of data is incomplete and further work is necessary.

A new charged particle detector configuration has been designed which should increase the sensitivity of the detector, previously used in the Harvard picosecond facility, by three orders of magnitude. The photoemission from silicon by UV probe pulse $\lambda = 262$ nm, will be investigated, as a function of the delay time from a 532 nm pump pulse which creates an electron-hole plasma. These experiments will complement the optical probe experiments of the project II-4.

II.6 Multiphoton Vibrational Excitation of Molecules. T.B. Simpson, E. Mazur, N. Carlson, I. Burak, and N. Bloembergen, Contracts N00014-75-C-0648 and DAHG29-81-K-0071; Research Unit 6.

The infrared multiphoton excitation of large molecules has been studied extensively over the last years. We have concentrated our efforts on small molecules. Although it is obvious that diatomic molecules cannot be excited by monochromatic infrared radiation in the absence of collisions, not much can be said about the behavior of diatomic and other small polyatomic molecules.

Following our previously reported work on CCS, the molecules NO_2, SO_2, DN_3, HN_3 and BCl_3 have been investigated. It was demonstrated that all, except NO_2 and OCS, do undergo collisionless infrared multiphoton excitation with short (100 ns - 0.5 ns) CO_2 laser pulses of high intensity (10 GW/cm^2) and fluence (100 J/cm^2). Energy deposition was measured photoacoustically, while dissociation was monitored and studied by spectral and temporal analysis of the chemiluminescence occurring after dissociation. It was found that the peak laser intensity plays an important role, while for larger molecules the total fluence density is the determining factor. High intensities are needed, because in small molecules coherent multiphoton processes must help overcome vibrational anharmonicities. The results clearly showed that the infrared multiphoton excitation of small molecules cannot be explained on the basis of a limiting process in the quasi-continuum of states.

In the case of DN_3 a whole chain of reactions takes place after dissociation. The photochemistry has been studied in detail for this molecule and a comprehensive paper has been prepared.[1]

The intramolecular vibrational energy transfer can be studied in a novel way by exciting the molecule first with a CO_2 laser pulse in an

infrared active mode, and subsequently probe the excitation of a Raman-active mode by anti-Stokes Raman spectroscopy. This method was pioneered by a research group in the spectroscopy laboratory of the Moscow Academy of Sciences in 1980, but has not been duplicated or improved upon anywhere else. Our 10 ns probe pulse from the second harmonic of a ruby laser will produce anti-Stokes radiation, whose photons will be detected in a multi-channel analyzer with sub-nanosecond time resolution, following the excitation of the molecule by a 100 picosecond CO_2 laser pulse. A gas cell with very low spurious light scattering has been built and the experimental apparatus is nearly assembled. A systematic study of the excitation of the 800 cm^{-1} Raman active mode in SF_6 is planned, as a function of energy fluence of the pump pulse and time delay.

Reference

1. T.B. Simpson, E. Mazur, K.K. Lehmann, I. Burak, and N. Bloembergen, "The Infrared Multiphoton Excitation and Photochemistry of DN_3," submitted to *J. Chem. Phys.*

II.7 Infrared Multiphoton Excitation of Excited Electronic States in Molecules. I. Burak, T.B. Simpson, E. Mazur, and N. Bloembergen, Contracts N00014-75-C-0648 and DAHG29-81-K-0071; Research Unit 7.

Infrared-visible double resonance studies of NO_2 have been completed. NO_2 molecules, excited by a visible laser pulse, were excited further by high power CO_2 laser pulses. Due to a breakdown of the Born-Oppenheimer approximation, states of the excited electronic manifold are well mixed with states of the ground electronic manifold. This makes it possible to directly populate highly excited vibrational states with the visible laser

pulse and probe for the existence of a "quasicontinuum" of levels with the infrared pulse. A systematic study of the fluorescence emitted by NO_2 molecules excited by the visible pulse yielded the first absorption and stimulated emission cross-sections for infrared pumping of such an excited molecule. Laser pulse intensity as well as fluence plays an important role in the infrared multiphoton excitation process up to the dissociation limit showing that NO_2, with only 3 normal vibrational modes, has no true "quasicontinuum" of vibrational energy levels. A comprehensive report on these results has been published.[1] This work was also presented at the International Conference on Quantum Electronics, Munich, June 1982.

Work in progress on SO_2 has yielded the first conclusive evidence for collisionless infrared multiphoton excitation of a triatomic molecule to an excited electronic state. Like NO_2 the states of the excited electronic manifold are mixed with highly excited states of the ground electronic manifold. Through the process of inverse electronic relaxation SO_2 molecules excited up through the vibrational ladder pass into the manifold of the excited electronic state and fluorescence. The observation of this fluorescence is also the first conclusive evidence that an isolated molecule with only three normal vibrational modes can absorb more than 30 infrared photons. Unlike larger polyatomic molecules, however, it is peak laser intensity and not laser fluence that governs the excitation process.

Reference

1. J.Y. Tsao, T.B. Simpson, N. Bloembergen, and I. Burak, "The Dynamics of the Infrared Multiphoton Pumping of Optically Excited NO_2 Molecules," *J. Chem. Phys.* 77, 1274 (1982).

III. INFORMATION ELECTRONICS CONTROL AND OPTIMIZATION

Personnel

Prof. R.W. Brockett
Prof. C.I. Byrnes
Prof. Y.C. Ho
Prof. R. Suri
Dr. T.S. Chang
Dr. P. Crouch
Dr. B. Tolwinski
Mr. A. Bloch
Mr. X. Cao
Mr. B. Ghosh
Mr. N. Gunther
Ms. V. Haimo
Mr. J. Loncaric
Mr. A. McIvor
Mr. N. Papageorgio
Mr. S. Peck
Ms. B. Sanders
Mr. L. Servi
Mr. T. Taylor
Mr. Z-J. Yang
Mr. Y-P. Zheng

III.1 Stabilization. R.W. Brockett, Contract N00014-75-C-0648; Research Unit 8.

A central problem in control theory is that of stabilizing a system with respect to a desired equilibrium point. For linear systems this is usually accomplished by traditional servomechanism techniques or else, especially in the multivariable case, by formulating an appropriate least squares problem and solving for the optimal control in feedback form. Underlying these results on linear systems is a simple principle: if the system is fully controllable then there exists a stabilizing feedback control law. There has never been a satisfactory version of this theory applicable to nonlinear systems. In our recent paper,[1] we show that the analogous principle is invalid by constructing a large class of fully

controllable systems which cannot be stabilized by feedback. The results given there identify a subclass of nonlinear systems for which the principle is valid and describe a method for constructing suitable feedback control laws in these cases.

Reference

1. R.W. Brockett, "Asymptotic Stability and Feedback Stabilization," in *Differential Geometrics in Control Theory* (R.W. Brockett *et al.*, eds.), Progress in Mathematics, vol. 27, Birkhäuser Publishers, Boston, MA, pp. 181-191, 1983.

III.2 Diffusion Equations in Control. R.W. Brockett, Contract N00014-75-C-0648; Research Unit 8.

This work is devoted to the analysis of a diffusion process which is prototypical of a class of diffusions which arise in nonlinear control systems subjected to stochastic inputs. These diffusions are poorly approximated by the Gauss-Markov processes. The optimal control properties of these control systems have been studied by us earlier.[1,2] In Ref. 3, the behavior of the diffusions is analyzed with particular attention being paid to the connection between them and the small time behavior and the optimal performance measured computed in Ref. 1. These results generalize a relationship which is well known in the case of Brownian motion; however, this generalization is somewhat subtle. For instance, in certain directions these "nonlinear" diffusions behave much more erratically than the usual n-dimensional Brownian motion and this qualitative difference must be related to the properties of the system.

References

1. R.W. Brockett, "Control Theory and Singular Riemannian Geometry," in *New Directions in Applied Mathematics* (P. Hilton and G. Young, eds.), Springer-Verlag, 11-27, 1981.

2. N. Gunther, "Hamiltonian Mechanics and Optimal Control," Ph.D. Thesis, Harvard University, 1982 (unpublished).

3. T. Taylor, "Hypoelliptic Diffusions," Ph.D. Thesis, Harvard University, 1983 (to appear).

III.3 Linear Systems. R.W. Brockett, Contract N00014-75-C-0648; Research Unit 8.

The computational problems associated with linear time invariant systems include the determination of the eigenvalues of the matrix describing the closed-loop behavior of the systems. In our recent paper,[1] we analyze the intrinsic complexity of carrying out this calculation and relate the complexity to the various symmetries of the root-locus diagram. We find, somewhat surprisingly, that the complexity of the eigenvalue determination problem is closely related to the properties of a parameterically excited feedback problem through some results in theory of Lie algebras.

Reference

1. R.W. Brockett, "Linear Feedback Systems and the Groups of Lie and Galois," *Linear Algebra and Its Applications*, vol. 24, 1983.

III.4 Credibility and Rationality of Strategies in Multi-Level Games. Y.C. Ho and B. Tolwinski, Contracts N00014-75-C-0648 and NSF-ENG78-15231, Research Unit 9.

A class of multi-level multi-person decision problems known as Stackelberg or incentive control problems involves two or more players, with one of them, often referred to as the leader, being in the position to declare his strategy before the others. When these strategy can be made to depend on other players' decisions, the possibility of threat or incentive control becomes significant. A basic tenet of incentive control assumes that the followers, the players other than the leader, believe that the leader is committed to his threat if the circumstances arise in which he claims he would use it. This credibility assumption is sometimes open to question particularly in cases where carrying out the threat may also be harmful to the leader. In this work, we address the question of rationality underlying the realization of the leader's threat and their credibility to the followers in the context of a simple two person game repeated over a period of time. The proposed model assumes that the credibility of the leader's threat as perceived by the follower is described in probabilistic rather than deterministic terms, and that this credibility is shaped by the leader's past record of keeping his word. The optimal solution for the leader is to carry out his threat depending on the circumstances but often enough to be consistent with the perception of the followers.

Reference

1. Y.C. Ho and B. Tolwinski, "Credibility and Rationality of Players' Strategies in Multi-Level Games," Proc. of 1982 IEEE Conferences on Decision and Control, Florida, December 1982.

I. SOLID STATE ELECTRONICS

Personnel

Prof. H. Ehrenreich
Prof. Choochon Lee
Prof. W. Paul
Prof. P.S. Pershan
Prof. M. Tinkham
Asst. Prof. C.J. Lobb
Dr. G.E. Blonder (till 8/82)
Dr. D.J. Frank (till 11/82)
Dr. F. Habbal (till 11/15/82)
Dr. P.B. Kirby
Dr. T.M. Klapwijk (visitor)
Dr. A. Lachter
Dr. M. Octavio (visitor, fall 1982)
Dr. S. Oguz
Dr. B. von Roedern
Dr. L. Sorenson
Dr. A. Weiss
Dr. B.G. Yacobi
Mr. J.M. Aponte
Mr. K. Chan
Mr. E. Chason
Mr. J. Collett
Mr. W.C. Danchi
Mr. J. Eggert
Mr. M.G. Forrester
Mr. K.C. Hass
Mr. Q. Hu
Mr. R. Lempert
Mr. E. Sirota
Mr. B. Velický
Mr. R. Weisfield
Ms. A.E. White

I.1 Electronic Structure of Disordered Semiconductors. H. Ehrenreich, K.C. Hass, and R. Lempert, Contract N00014-75-C-0648; Research Unit 1.

In last year's proposal we reported the results of preliminary coherent potential approximation (CPA) calculations of the electronic structure of $Hg_{1-x}Cd_xTe$.[1] These were based on an empirical LCAO approach and the HgTe and CdTe tight-binding parameters of Czyżyk and Podgórny. The result clearly demonstrated that strong scattering due to cation s level disorder occurs low in the valence band of $Hg_{1-x}Cd_xTe$, in agreement with photoemission experiments.

Recently we have provided a much more complete analysis of disorder effects in $Hg_{1-x}Cd_xTe$ using additional CPA calculations based on a more reliable set of tight-binding parameters.[2] The results for the valence and conduction band density of states, the bowing of the fundamental gap with composition and those for the gap at L are in good agreement with experiment. In addition, we find that the damping near the band edges is indeed weak and in particular that the electron mobility should be very high (in excess of 100,00 cm^2-volt/sec for compositions of interest in infrared detectors). Furthermore, the fundamental of optical absorption edge should closely resemble that of a pure crystal. The tight-binding scheme used in these calculations involves non-overlapping orbitals and empirically adjusted hopping integrals. Interactions with second nearest neighbors as well as spin-orbit effects are included. Disorder is treated within the coherent potential approximation and for that reason is confined to the atomic energies of the individual constituents. The latter are determined from self-consistent relativistic Hartree-Fock calculations. The effects of disorder on the hopping integrals are treated within the virtual crystal approximation. The parameters are adjusted by using self-consistent band structure results for pure parent compounds, optical data, and some aspects of Harrison's universal tight-binding scheme. The programs that have been developed to date apply to alloys derived from a zincblende structure. They have been thoroughly checked against existing calculations.

During the coming year we expect to generalize the programs to apply to materials having disorder on both sub-lattices of the zincblende structure. While this generalization is simple in principle, it may be that the time required for the necessary computations is too great. For this reason, the implementation of this technique must depend on simplifying

assumptions and symmetry properties that will permit reduction of the size of the 8×8 matrices that arise in these calculations. We would in any case expect to apply this procedure to materials having anionic disorder such as Ga(As,P) in order to ascertain the effects of such disorder on the valence band edges. Since it may also be possible to prepare GeSn in a metastable form for compositions in excess of those permitted by the phase diagram, it will be of interest to investigate the electron structure of this material, because it too promises to have a high electron mobility for compositions when the conduction band minimum lies at $k = 0$. Finally, we hope to take at least a preliminary look at the ternary 3-5 alloys.

References

1. H. Ehrenreich and K.C. Hass, *J. Vac. Sci. Technol.* 21, 133 (1982).

2. K.C. Hass, H. Ehrenreich, and B. Velický, *Phys. Rev.* B27, 1088 (1982).

I.2 Electronic Structure of $Hg_{1-x}Mn_xTe$.

K.C. Hass and H. Ehrenreich, Contract N00014-75-C-0648; Research Unit 1.

The approach described above has been extended to apply to the electronic structure of $Hg_{1-x}Mn_xTe$.[1] This alloy has recently attracked considerable attention both for its interesting magnetic properties, and as a possible alternative to $Hg_{1-x}Cd_xTe$ for use in infrared devices. Our picture of the electronic structure of $Hg_{1-x}Mn_xTe$ is believed to be the first. Its development utilizes all relevant experimental information, atomic energy levels, and previous experience with both tight-binding theory and the CPA. The results are in substantial agreement with presently

available experimental results. While the approach to the problem used here is simple, a better, fundamentally-based but far more complicated alloy calculation, while certainly worthwhile, would not necessarily sharpen qualitative physical insight.

Before the same approach can be applied to $Hg_{1-x}Mn_xTe$, two complicating factors must be taken into account. First, good quality zincblende crystals of $Hg_{1-x}Mn_xTe$ can only be formed for $x \lesssim 0.3$; the limiting crystals HgTe and MnTe do not exist in the same crystal structure. The second complication is the presence of spin-polarized half-filled shells of Mn d electrons, which are responsible for the interesting magnetic effects in $Hg_{1-x}Mn_xTe$. Their contribution to the electronic structure of this material has not been extensively discussed.

To overcome these difficulties we first obtain a set of s and p electron tight-binding parameters for a hypothetical zincblende form of MnTe. These parameters are then used in conjunction with the HgTe parameters and CPA formalism of Ref. 1 to calculate the s-p electron "complex band structure" of $Hg_{1-x}Mn_xTe$ in the absence of interactions with Mn d electrons. The effects of (s-p)-d interactions, to a good approximation, can be taken into account in perturbation theory.

As in $Hg_{1-x}Cd_xTe$, most of the essential physics of $Hg_{1-x}Mn_xTe$ can be understood directly from a consideration of the diagonal tight-binding parameters in the limiting crystalline compounds. In zincblende MnTe these parameters are determined from atomic energy elevels in the same way as that used to find the HgTe and CdTe diagonal levels in Ref. 2. This approach has the attractive feature of ensuring that the most important parameters are consistently determined and structurally independent.

The effects of disorder due to the cation s levels is about twice as great in the Mn alloy. As a result the split band behavior low in the valence bands is more pronounced than in HgCdTe. The disorder-induced bowing or nonlinear variations of band gaps with compositions is described well within the CPA. For the gap associated with the E_1 transition, the virtual crystal approximation is particularly bad in HgMnTe. The CPA appears to account well for this variation.

The Mn d electrons in HgMnTe and CdMnTe are degenerate with the valence band and have usually been assumed to be strongly localized. By contrast, photoemission experiments have indicated that there may be considerable dispersion in the band. Thus, the d electrons may well be itinerant as in the transition metals. The degree of hybridization with the valence bands can be estimated in similar ways as that used in previous work on transition metals. Numerical estimates indicate that the predicted d band width is approximately that conjectured from the interpretation of the experiment but that the d electrons have little effect on the band edge states important for device applications. Of particular interest is the already noted fact that the occupied levels are spin-polarized. Thus in the anti-ferromagnetic and spin glass states itinerant electrons are such that their spins vary from site to site. Since we have worked fairly extensively on electronic structures of semiconductors, transition metals, and alloys we find the present research on the semimagnetic semiconductors of particular interest since it represents the synthesis of the theories used to describe both types of material and substitutional alloys.

Possible future extensions of this work will include (1) applications to other semimagnetic semiconductors, particularly CdMnTe; (2) development of a model Hamiltonian approach which will be useful in studying the

interplay between magnetic and alloying effects; (3) applications to ordered or disordered magnetic systems such as itinerant anti-ferromagnets. In this connection it should be noted that recent theoretical work indicates that even materials such as MnO contain d electrons that are itinerant.

References

1. K.C. Hass and H. Ehrenreich, *J. Vac. Sci. Technol.* (to be published, 1983).

2. K.C. Hass, H. Ehrenreich, and B. Velický, *Phys. Rev.* B27, 1088 (1983).

I.3 Simplification of Green's Function Calculations. K.C. Hass, B. Velický, and H. Ehrenreich, Contract N00014-75-C-0648; Research Unit 1.

A novel approach that greatly simplifies integrations over the Brillouin zone which are associated with most of the difficulties encounted in numerical implementation CPA alloy calculations, were developed about a year ago. This approach has been implemented throughout the calculations reported in earlier parts of this report. A full account of this work is in preparation.[1] Its delay in publication is due in part to our burgeoning interest in the semimagnetic semiconductors and the need to verify, as has now been done, that the method is indeed as versatile and accurate as we had originally surmised.

Reference

1. K.C. Hass, B. Velický, and H. Ehrenreich (to be published).

I.4 Optical Properties of Disordered Semiconductors. K.C. Hass and H. Ehrenreich, Contract N00014-75-C-0648; Research Unit 1.

Last year's report described work in progress concerning the calculation of the frequency-dependent dielectric function for interband transitions in disordered semiconductors. The otpical properties of disordered systems differ from those of crystals in the breakdown of k-conservation, the existence of vertex corrections of a kinematic kind which produce correlations between electrons and holes, and the effects of random momentum matrix elements. This work has essentially remained dormant during the past year with one exception: it now appears that the so-called "Urbach tail effects" are associated with random fluctuations in the lattice due to either phonons or impurities and that these are well described within the framework of the CPA. Much of this work has already been summarized in draft form and we hope to complete it during the coming year.

I.5 Spatial Decay of the Nonequilibrium Potential in Phase-Slip Centers. J.M. Aponte and M. Tinkham, Contract N00014-75-C-0648 and NSF Grant DMR-79-04155; Supplementary Unit.

We have measured the spatial decay of the chemical potential of the quasiparticles generated in a phase-slip center (PSC).[1] Our samples are tin microbridges ($40\mu \times 1\mu \times 0.1\mu$) with four tunnel junction probes, fabricated photolithographically. When the current along the microbridge exceeds the critical current of the weakest point, a PSC is formed and a potential difference between the pairs and the quasiparticles appears. In our samples the central section of the microbridge is narrower than the rest of the microbridge in order to assure the nucleation of a PSC in that

location. The nonequilibrium potential is detected by measuring the voltage between each normal probe and one end of the microbridge. We have observed that this potential decays exponentially with the distance from the center of the PSC. The characteristic length Λ_{Q^*} diverges at T_c following the relation $\Lambda_{Q^*}(T) = \Lambda_{Q^*}(0)(1-T/T_c)^{-1/4}$ which corresponds to the relaxation time of the branch imbalance mode of disequilibrium $\tau_{Q^*}(T) = 0.73\tau_E\Delta(0)/\Delta(T)$. From the magnitude of $\Lambda_{Q^*}(0)$ we obtained the inelastic scattering time $\tau_E = (1.6 \pm 0.4) \times 10^{-10}$ sec. This value agrees well with our previous result[2] obtained in measurements of the interaction between two PSCs via quasiparticle current and it also agrees with values found in the literature.

In another type of experiment, we have detected the Josephson oscillations in the core of the PSC by observing the current steps in the I-V curves of microwave irradiated tin microbridges. We found that this effect depends on the length of the microbridge. Well defined Josephson steps were observed in samples up to 10 μm long.

References

1. W.J. Skocpol, M.R. Beasley, and M. Tinkham, "Phase-Slip Centers and Nonequilibrium Processes in Superconducting Tin Microbridges," *J. Low Temp. Phys.* 16, 145 (1974).

2. J.M. Aponte and M. Tinkham, "Spatial Decay of the Quasiparticle Current in Phase-Slip Centers," to appear in *J. Low. Temp. Phys.* 51, 189 (1983).

I.6 I-V Curves of Point Contacts. G.E. Blonder, M. Octavio, T.M. Klapwijk, M. Tinkham, Contract N00014-75-C-0648 and NSF Grant DMR-79-04155; Supplementary Unit.

Recently we presented a theory of the subharmonic gap structure observed in superconducting metallic contacts, based on repeated Andreev reflections at the two "banks" connected by a (normal) metallic "bridge" across which the voltage is developed. Subsequently we gave a more detailed analysis[2] of the N-S interface including an adjustable barrier potential there to model thin oxide layers, etc. The resulting predictions for I-V curves as function of temperature and barrier height have now been tested experimentally[3] and found to give a very good account of the variety of data taken with a Nb-Cu point contact system, ranging from the high-barrier ("tunnel junction") limit to a clean metallic contact in which the only "barrier" results from the change in Fermi velocity in crossing from Nb to Cu. Encouraged by these results, we have carried out computer calculations[4] of the subharmonic gap structure in a superconducting link, which for the first time also include scattering processes represented by weak barrier potentials at the interfaces. These calculations confirm that a small amount of scattering is sufficient to cure an apparent failure in the model without scattering, namely, the predicted disappearance of the effect as $T \to 0$. A realistic amount of scattering not only generally enhances the magnitude of the structure, but also brings the predicted temperature dependence into line with experimental data. Given this new theory, we are presently starting a new set of experiments on contacts under conditions for which our theory should be particularly exactly applicable. These results should provide a rather decisive test of our model in comparison with several others which have been advanced.

References

1. T.M. Klapwijk, G.E. Blonder, and M. Tinkham, Invited Paper at LT16 Conferences in Los Angeles, August 1981; *Physica* 109, 110B, 1657 (1982).

2. G.E. Blonder, M. Tinkham, and T.M. Klapwijk, *Phys. Rev.* B25, 4515 (1982).

3. G.E. Blonder and M. Tinkham, *Phys. Rev.* B27, 112 (1983).

4. M. Octavio, M. Tinkham, G.E. Blonder, and T.M. Klapwijk, *Phys. Rev.*, submitted.

I.7 Production and Characterization of Amorphous Semiconductors. P. Monagle, S. Oguz, B. von Roedern, R. Weisfield, and W. Paul, Contracts N00014-75-C-0648, NSF-DMR-81-08327 and SERI subcontracts XW-1-9358-1 and XB-2-02144-1 of DOE prime contract EG-77-C-01-4042; Research Unit 3.

We have continued to make amorphous semiconducting films of Si, $Si_{1-x}H_x$, Ge, $Ge_{1-x}H_x$ and $Si_{1-x-y}Ge_xH_y$ by two methods: (1) r.f. sputtering of crystalline targets by Ar onto substrates of Corning 7059 glass, fused silica, Al and c-Si held at temperatures between 0°C and 400°C. The preparation parameters varied have been the substrate temperature T_s, the partial pressure of H_2, and the r.f. power; (2) by glow-discharge decomposition of SiH_4, GeH_4 and appropriate mixtures of these gases with H_2. A new design of glow-discharge apparatus, incorporating provisions for a better vacuum, gas monitoring by residual gas analyzer, improved gas flows and plasma confinement, has been built and tested through the production of device-quality a-$Si_{1-x}H_x$.

The films are analyzed chemically by electron microprobe; X-rays are used to verify amorphicity or to determine the presence and size of microcrystals. SEM examination provides information on a certain scale of structure. The film thickness is determined by a Sloan Dektak profile-meter or by edge-on viewing in the SEM. The relative H-contents are determined from the integrated area of the X-H wagging mode vibrational absorption near 500-600 cm^{-1}.

Following our now standard procedure, co-deposited films are used for measurements of electrical conductivity versus temperature, photoconductivity under fixed illumination, photoconductivity spectrum to give the low energy optical absorption spectrum, photoluminescence, optical absorption, drift mobility and some measurement designed to give an estimate of the gap density of states near the middle of the optical gap. Then a self-consistent model for the densities of states and the transport and recombination processes is sought.

In the following sections only the measurements supported, or partly supported, by the JSEP will be described. The measurements of field effect in amorphous semiconductors, time-of-flight mobility, and low photon energy photoconductivity spectra, initiated under the JSEP, are now carried out almost routinely, and are necessary for overall film evaluation, but receive their support from other agencies. The JSEP program support is directed toward the consequences of heterogeneity, improved short-range order, and crystallinity on a scale of the order of 50 Å for transport and phototransport. It is also directed toward improvement of measurements, on a time scale of nanoseconds, of transient photoconductivity, transient induced absorption and transient photoluminescence, which have direct bearing on steady state transport and phototransport in amorphous systems.

Finally, a new effort, to which the majority of JSEP funds has been directed, will be described: the investigation of the possible fabrication of crystalline films of $Ge_{1-x}Sn_x$ which would have a direct band gap tunable with x down to low values.

I.8 Transient Phototransport Measurements in a-Si:H. P.B. Kirby and W. Paul, Contracts N00014-75-C-0648 and DOE DE-AC02-82ER12064; Research Unit 3.

When carriers are photoexcited in a-Si:H, they first thermalize in extended band states above the mobility edges, a process which is complete on the order of picoseconds. Thereafter the carriers relax into tails of localized states, whose density is usually supposed to decrease exponentially with energy away from the band edges. Whether or not this functional variation of state density is accurate, the continuous density of states in the band tails leads to phenomena not usually seen in crystalline semiconductors. The carriers in the conduction band tails (on which we focus attention) are continually excited back into the conduction band states and are continually retrapped. Their distribution in energy sinks continuously to energies further and further from the band edge as time progresses. Since transport only takes place via the fraction of carriers above the mobility edge, the photocurrent decreases with time without there being any disappearance of carriers through recombination. This phenomenon is commonly referred to as dispersive transport, and the decay of photocurrent is (rather ambiguously) said to reflect a time-dependent mobility. In general terms, though, the photocurrent transient contains information about the distribution in energy of the localized states and their capture cross sections.

One method of studying transient phototransport is to arrange a sample with two electrodes in a sandwich configuration. The front contact is a rectifying one. A pulse of illumination (from a laser, usually) produces electrons and holes very near one electrode. The field applied sweeps one type of carrier immediately to the near electrode and the other down the sample to the second electrode, a considerable (relatively speaking) distance away. For this so-called time-of-flight configuration, a very general theory for the photocurrent transient, which does not, in fact, depend on the assumption of a multiple trapping model, gives expressions for the current:

$$I(t) \propto t^{-(1-\alpha_i)} \qquad t < t_T$$

$$I(t) \propto t^{-(1+\alpha_f)} \qquad t > t_T$$

where t_T corresponds approximately to the time when 50% of the carriers have traversed the sample to the back electrode. The transit time may be used, in combination with the known sample thickness and the applied field, to obtain a drift mobility. On the other hand, the parameters α_i and α_f give information about the nature of the transport process. For example, in the special case which probably applies to a-Si:H, it is a reasonable proposition, from a variety of experimental data, that the dispersive transport has its origin in multiple trapping in an exponentially distributed tail of localized states. In such a case α_i should equal α_f and α_i should be equal to T/T_c, where T is the temperature of measurement and T_c describes the exponential tail of states, $N(E) = N_0 \exp(-|E|/kT_c)$, below a mobility edge at $E = 0$.

Other photoinduced phenomena may be studied and correlated with the above. A particular experiment was done in which we collaborated with Professor Jan Tauc's group at Brown University. Tauc's group is expert in the measurement of photoinduced absorption in the time range covered by the time-of-flight measurement. The experiment consists of measuring the change in magnitude of the integrated absorption, at energies of about half the optical gap, as a function of time after an exciting pulse of radiation. At this stage it is supposed that the dominant contribution to this absorption is given by the photoproduced holes, but that, significantly, they disappear through recombination with the electrons whose transport to the site of the trapped hole is the rate-limiting process. Thus we may assume a time-dependent

rate coefficient for diffusion-limited bimolecular recombination of

$$b = B/t^{1-\alpha_i} \qquad (0 < \alpha < 1)$$

which leads to a time-decay of the induced absorption corresponding to a change in the fractional transmission

$$-\frac{\Delta T}{T} \propto t^{-\alpha_i} \quad .$$

The collaborative experiment carried out was to measure the α's from time-of-flight (Harvard) and induced absorption (Brown) on samples of a-Si:H produced by sputtering at Harvard and characterized as to all other significant parameters by us. The experiment showed a very satisfactory coincidence of the variation of [illegible] T from the two types of experiment, which served to validate, for the first time, several of the assumptions made to describe the [illegible] experiments.[1]

References

[1] P.G. Le Comber, W. Paul, S. Ray and J. Tauc, *Solid State Commun.* 42, 333 (1982).

I.9 Phototransients in a-Si:H and Bimolecular Recombination. P.B. Kirby and W. Paul, Contract N00014-75-C-0648; Research Unit 3.

An extensive set of photocurrent transients in a-Si:H, consequent on pulsed (nsec) laser excitation, were measured on samples in sandwich and coplanar geometry. Both glow-discharge produced and sputtered samples (see I.7) were studied. The measurements on sandwich structures, where a large applied field quickly separates the carriers and prevents electron-hole

recombination (although not deep trapping), may be used to determine a time-dependent mobility. This time-dependent mobility is attributed to shallow electron trapping in an exponential tail of states below the conduction band mobility edge. Measurements on coplanar structures, where a time-dependent mobility also pertains, but where the coexisting electron and hole distributions may lead to recombination, may then be interpreted to give information on the recombination processes.

It was found that in undoped a-Si:H bimolecular recombination dominates the measurements in coplanar geometry down to the lowest usable intensities of illumination--a new result. Moreover, the bimolecular recombination process appears to change with temperature. Faster recombination was usually observed in sputtered a-Si:H, presumably because of a different distribution of recombination centers compared to the glow-discharge material. Finally, phosphorus doping of the a-Si:H was found to lead to an increase in the recombination time, so that it has been possible to study both bimolecular and monomolecular recombination, depending on the incident light intensity. This result of P doping may be explained in terms of the complex circumstance that this dopant introduces both donor-like states near the conduction band edge (probably caused by four-fold coordinated P) and deep states in the lower half of the pseudogap (possibly caused by P-defect complexes, but this is less certain). The final outcome is effective trapping of the photoexcited hole and a lengthening of the electron lifetime, and this is reflected in the time-dependence of the electron-dominated transient photocurrent.

I.10 Metastable Semiconducting Alloys of $Ge_{1-x}Sn_x$. S. Oguz and W. Paul, Contract N00014-75-C-0648; Research Unit 3.

Crystalline germanium has an indirect band gap $(L_1 - \Gamma_{25'})$ of about 0.65 eV near room temperature, and a direct band gap $(\Gamma_{2'} - \Gamma_{25'})$ about 0.15 eV larger. Grey Sn (α-Sn) is a perfect semimetal, or semiconductor with zero band gap, caused by a degeneracy at the $\Gamma_{25'}$-point.[1] It is estimated that $\Gamma_{2'}$ lies about 0.4 eV below $\Gamma_{25'}$ and L_1 about 0.1 eV higher than $\Gamma_{25'}$.[1] A simple interpolation then shows that the alloy system $Ge_{1-x}Sn_x$ possesses a range of composition where the band gap is direct and is variable, with x, through zero. As a particular example, for $x = 0.4$ the predicted direct gap is approximately 0.4 eV. Such a material, if it could be made, would have obvious device applications and possibly be a good alternative to 3-5 and 2-6 compounds, whose mobilities are limited by polar scattering. Unfortunately, the phase diagram of Ge-Sn indicates that the solid solubility of either element in the other is less than 1% in crystals under equilibrium conditions. The stable phase of tin at room temperature (β-Sn) is a metal. It is worth considering, however, whether the equilibrium phases may be bypassed through the method of fabrication chosen and thus metastable diamond-structure semiconducting alloys formed.

Some ten years ago, we produced amorphous $Ge_{1-x}Sn_x$ with $0 \leqslant x \leqslant 0.5$ by sputtering pressed powder targets of Ge-Sn mixtures in argon onto substrates held near room temperature.[2,3] The objective at the time was to produce amorphous semiconductors of smaller pseudogap than a-Ge so that the transport properties could be pursued with ease to very low temperatures without there being created any problems of conductivity measurement. (Apparatus development since has probably solved this problem of measurement of low conductivities.) The restriction on x was not necessarily a vital one, since mixed

targets of larger x were not tried. The technique established, *inter alia*, that (1) amorphous, tetrahedrally-coordinated, truly random non-phase-separated alloys of $Ge_{1-x}Sn_x$ could be made, with $0 \leqslant x \leqslant 0.5$, and (2) the resultant amorphous semiconductors had reduced pseudogaps from a-Ge, and so higher conductivities. For our present purposes, however, a study of the effects of annealing was important.[3] It was established, through subsequent X-ray and electron microprobe examination, that it was possible to produce *crystalline* $Ge_{1-x}Sn_x$ with x much larger than 0.01. However, the converted films had included in them an intimately intermixed fraction of β-Sn on a scale of several hundred Å. This investigation was halted and subjected to a long postponement when the laboratory became fully involved in the study of the hydrogenation of amorphous semiconductors such as Ge and Si.

We have now returned to this investigation. Films of $a\text{-}Ge_{1-x}Sn_x$ have been made, by sputtering with Ar, targets of polycrystalline Ge with attached Sn. The use of pressed powder targets has been discontinued; while they assure uniform composition of the resulting film, it is almost inevitable that some gas, such as O, is incorporated during the powder sintering process. Also, we have found that when pressed powder targets (of any composition--Ge-Sn, Ge-Si, etc.) are sputtered in $Ar\text{-}H_2$ mixtures, the H is incorporated into the target, where it appears to catalyze subsequent uptake of a large amount of oxygen or water vapor.

The films of $a\text{-}Ge_{1-x}Sn_x$ are now annealed using a cw Ar-ion laser operated in an 'all-lines' mode and delivering 0-6 W power. The laser beam is focussed to a spot of ~160 μm diameter, and the sample, mounted on an x-y-z translator stage, is scanned across the spot at adjustable speeds. X-ray diffraction is used on films thicker than 1 μ to determine crystallinity, compositional homogeneity (actually a search for β-Sn peaks) and

crystallite size, from the width of the diffraction lines. Electron microprobe analysis is also employed to determine the film composition.

We have found that films of $Ge_{0.7}Sn_{0.3}$ deposited below a substrate temperature of about 120°C are amorphous, whereas at higher substrate temperatures they are polycrystalline and phase-separated. Optical measurements on the amorphous samples show that they have narrower bandgaps than a-Ge ($E_{04} \simeq 0.5$ eV, compared with about 0.8 eV), consistent with the earlier findings. The phase-separated, crystalline films are opaque, as expected.

The amorphous films have been subjected to laser annealing under several combinations of laser power and sample scanning speeds. Some of these lead to surface bubbling, beading, discoloration, etc., and to phase separation as revealed by X-rays. However, at low scan speeds and about 0.5 W power, X-ray measurements revealed that the intensity of the β-Sn peaks was very much reduced (actually barely detectable through noise) while the Ge (111) X-ray diffraction peak was shifted by the effect of alloying. A linear interpolation between the lattice parameters of c-Ge and c-Sn suggested a composition of 85% Ge, 15% Sn, while the width of the X-ray diffraction corresponded to crystallite of the order of 100 Å in size. An electron microprobe study showed no inhomogeneity within a 1 µm spot size. Optical transmission measurements showed that the film was opaque. This is interpreted to mean that, even although there is hardly any β-Sn signal, nevertheless the extra Sn (the crystal composition is 0.15, the target 0.30) must be distributed in very small volumes, agglomerated enough to make the material opaque.

We conclude that this approach holds sufficient promise that other conditions of varying x in the target, and altering the annealing laser's power and dwell time, should be attempted.

In parallel with this approach, we have begun to investigate the possibility that crystalline *alloy* films may be deposited directly by the sputtering method if the substrate is chosen to approximately match the lattice constant of the depositing *crystalline* alloy. Such a general approach has been adopted at RSRE, and workers there have succeeded in depositing *crystalline* α-Sn on InSb by MBE at substrate temperatures of about 25°C, as long as the films are kept thin ($\leqslant 0.5\ \mu$). The lattice mismatch between α-Sn and InSb is about 0.2%. Our modified approach is very simply to choose a different substrate, such as InAs or InP, for the deposition of Ge-Sn alloy. Whether this can be done by the sputtering method is open to question, and in fact the very good vacuum conditions of MBE apparati may be needed for success. While we do not expect this approach to be without pitfalls, it should be noted that the success at RSRE of maintaining the metastable α-Sn at a temperature, 70°C, some 60°C higher than the conversion temperature to β-Sn, suggests that Ge-Sn may also be so stabilized.

References

1. S.H. Groves and W. Paul, *Phys. Rev. Lett.* 11, 194 (1963).

2. R.J. Temkin, G.A.N. Connell and W. Paul, *Solid State Commun.* 11, 1591 (1972); N.J. Shevchik and W. Paul, *J. Non-Cryst. Solids* 13, 1 (1973); G.A.N. Connell, R.J. Temkin and W. Paul, Proc. of Fifth Int. Conf. on Amorphous and Liquid Semiconductors, Garmisch-Partenkirchen 1973 (Taylor and Francis, 1974), p. 1201.

3. R.J. Temkin and W. Paul, Proc. of Fifth Int. Conf. on Amorphous and Liquid Semiconductors, Garmisch-Partenkirchen 1973 (Taylor and Francis, 1974), p. 1193.

4. R.F.C. Farrow *et al.*, *J. Cryst. Growth* 54, 507 (1981).

I.11 X-Ray Scattering in Liquid Crystals. J. Collett, K. Chan, E. Sirota, L. Sorensen, and P.S. Pershan, Contracts N00014-75-C-0648, NSF-DMR-80-20247 and NSF-DMR-82-12189; Research Unit 4.

X-ray scattering studies of structural phase transitions in freely-suspended smectic liquid crystal films have been continued. This particular project is primarily supported by the NSF under grants DMR-79-19479 and DMR-80-20247. However, it receives ancillary support from JSEP and is directly related to other X-ray projects supported by JSEP. Initial studies on the material 70.7 were described in last year's progress report. A *Physical Review Letter* describing those results was published during the present year.[1] In the current report period we have carried out similar studies on thick films of materials 50.6 and 90.4. Restacking transitions similar to those observed in 70.7 were confirmed in 50.6. In addition, however, 50.6 was shown to exhibit a hexagonal phase with ABC stacking. Both 50.6 and 90.4 are also known to have smectic-F phases. These are particularly interesting in that there is long range order in the direction of the molecular tilt but there is only short range order in molecular positions.

During the report period we requested and obtained time on the high flux beam line V-II at the SSRL (Stanford) laboratory in order to investigate the manner in which these phases change as the films are reduced to thicknesses that correspond to only a few layers. The first experiment attempted in December of 1982 indicated the need for certain technical changes in the design of our oven in order to take into account differences in the physical properties of thin and thick films.

We are also in the process of constructing a second oven that can be used with an optical microscope to characterize certain thin film properties. In particular, this oven is designed to allow independent control of both

temperature and relative humidity. The latter is most important for our proposed future studies on lyotropic liquid crystals.

A second synchrotron X-ray experiment was carried out at the HASYLAB in Hamburg, Germany. In the last report period we described a new technique for carrying out X-ray studies of a horizontal liquid-gas interface. The first results of that experiment were published this year.[2] Those experiments were continued and further synchrotron runs were made in June and December of 1982. The most striking singular result of those studies was that the reflectivity of 8K eV X-rays from the horizontal liquid crystal surface was monitored from grazing incident angles up to angles of the order of 3° away from grazing incidence. In this range the reflectivity fell by seven orders of magnitude in a manner that could be explained theoretically with a minimum number of adjustable parameters. In particular, as a result of smectic order that appears near the surface of the nematic phase, the reflectivity had a structure that was the result of Bragg-like reflection. The line shape for this peak in the reflectivity was shown to be the consequence of constructive and destructive interference between normal specular reflection and the Bragg-like reflection from the smectic layers. Measurement of the relative intensity of the Bragg-like reflections and the specular reflections show promise of obtaining an absolute measure of the smectic order parameter. Theoretical analysis of these results are in process.

As a result of this study we now believe it is possible to study the structure of a broad class of liquid-vapor interfaces. We are currently exploring these possibilities theoretically and we hope to initiate an experimental program to take advantage of this discovery in the next year or two.

We have begun a series of X-ray measurements to characterize a new type of smectic-A liquid crystal in which there appear to be two incommensurate

density waves with independent thermodynamic properties.[3] These materials are characterized by a high temperature nematic phase in which there are two diffuse X-ray peaks at scattering vectors which are near to being in the ratio of 2:1 (i.e., one is nearly the second harmonic of the other). As the temperature is cooled down, different materials will have one of the following behaviors: 1) the fundamental condenses while the second harmonic remains diffuse, 2) the second harmonic condenses while the fundamental remains diffuse, or 3) in some cases it is believed that both condense at the same time. On further cooling, in either of the first two cases, the second diffuse peak will also condense and when that happens there will be a locking together of the two density waves such that one becomes exactly the second harmonic of the other. We have performed an initial set of measurements on two compounds. In one case, the second harmonic condenses first with a temperature dependence that is similar to the temperature dependences one finds in more normal nematic to smectic-A phase transitions. At a much lower temperature the fundamental condenses. Preliminary analysis suggests that the temperature dependence by which the fundamental condenses when the second harmonic is already condensed is both qualitatively and quantitatively different than the more normal nematic to smectic-A phase transition. We are in the process of analyzing this system in order to test various theoretical models.

A second system that we have studied was the fundamental condensing first. Further cooling down exhibits a sharp peak that is the second harmonic of the fundamentl co-existing with a broad diffuse peak that is not quite centered on the second harmonic. On further cooling the broad diffuse peak gets drawn into the second harmonic in a way that is reminiscent of the phase locking of two oscillators in the time domain.

Both theoretical analysis and further experiment on both of these systems is required.

References

1. J. Collett, L.B. Sorensen, P.S. Pershan, J. Litster, R.J. Birgeneau, and J. Als-Nielsen, *Phys. Rev. Lett.* 49, 553 (1982).

2. J. Als-Nielsen, F. Christensen, and P.S. Pershan, *Phys. Rev. Lett.* 48, 1107 (1982).

3. F. Hardouin, M. Levelut, and G. Sigaud, *J. de Phys.* 42, 71 (1981); G. Sigaud, F. Hardouin, M.F. Achard, and M. Levelut, *J. de Phys.* 42, 107 (1981).

I.12 Light Scattering From Thin Smectic Films. M. Sefton, L. Sorensen, and P.S. Pershan, Contracts N00014-75-C-0648, NSF-DMR-79-19479; Research Unit 4.

Progress in this project has been resumed with a new student. An oven has been constructed, electronics have been assembled and measurements will resume in the late winter or spring of 1982-1983.

I.13 Critical Elastic Properties of Free Surface Samples at the Nematic to Smectic-A Phase Transition. M. Fisch, L. Sorensen, and P.S. Pershan, Contracts N00014-75-C-0648, NSF-DMR-79-23597 and NSF-DMR-79-19479; Research Unit 4.

The principal experimental results obtained from this project were described last year. One publication that was in preparation last year has now appeared[1] and a second longer manuscript is in preparation.

Reference

1. M.R. Fisch, L.B. Sorensen, and P.S. Pershan, *Phys. Rev. Lett.* 48, 943 (1982).

II. QUANTUM ELECTRONICS

Personnel

Prof. N. Bloembergen
Prof. T.W. Mossberg
Dr. I. Burak
Dr. N.W. Carlson
Dr. C.D. Cordero
Dr. H. Kurz
Dr. L.A. Lompre
Dr. E. Mazur
Mr. M.C. Downer
Mr. J.M. Liu
Mr. L. Rothberg
Mr. T. Simpson
Mr. A.G. Yodh

II.1 Nonlinear Four-Wave Mixing in Vapors. M. Downer, L. Rothberg, and N. Bloembergen, Contract N00014-75-C-0648; Research Unit 5.

Low resolution studies of collision-induced four-wave mixing, reported in previous annual progress reports, have demonstrated the correct formalism to account for damping in nonlinear quantum mechanical processes. A brief review of this early work has been published. The detailed behavior of the intensities and lineshapes of collision-induced resonances in four-wave mixing has now been investigated at high resolution ($\lesssim$ 1 MHz).

One thrust of our studies in the past year has been to investigate the effects of level degeneracies on four-wave mixing in sodium vapor induced by collisions with He buffer gas. When the beams contributing to coherent absorption (ω_1) and emission (ω_2) have mutually orthogonal polarization, collision-induced Raman type resonances between Zeeman sublevels of the ^2S ground state of sodium occur. In the absence of a magnetic field, four-wave

collision-induced Raman type resonances between Zeeman sublevels of the ^2S ground state of sodium occur. In the absence of a magnetic field, four-wave mixing enhancements occur when the difference frequency $|\omega_1 - \omega_2|$ is near zero or near the hyperfine splitting of the ground state ($\sim$ 1.8 GHz). The homogeneous width of these lines is predicted to be determined by the spin exchange rate which relaxes the ground state, and should be about 1 MHz at the sodium pressures used. The observed linewidths are in fact determined by the collisionally narrowed residual Doppler broadening due to the small angle between input beams.

The splitting of these collision induced resonance lines has been observed. These experimental results on collision induced Zeeman coherence were first reported at the 8th International Conference on Atomic Spectroscopy held in Gothenburg, Sweden, August 1982, and will be published in the Proceedings.[2]

If the beams at ω_1 and ω_2 have parallel polarizations, their fields interfere giving rise to a population grating resonance in four-wave mixing when their frequencies are nearly equal so that the populations can follow the intensity modulation in time. Due to optical pumping of the ground state, the grating formed by collisional absorption relaxes with components due to excited ^2P state relaxation back to equilibrium. The component of homogeneous width 20 MHz ($\equiv 1/T_{1,sp}$) corresponding to the excited state spontaneous emission rate of sodium is broadened by quenching of the ^2P population by collisions with N_2. The removal of the excited state grating by the addition of N_2 gas leaves a residual resonance of essentially the inhomogeneous width (as low as 5 MHz) which we attribute to a ground state grating due to optical pumping. The mechanism of this optical pumping is not yet completely understood.

Preliminary studies of collisional narrowing in different buffer gases have been performed to investigate the properties of velocity-changing collisions which cause this phenomenon. Also, studies are in progress to determine how these resonances are modified at large detuning from the sodium D lines where the impact approximation breaks down. A paper incorporating our most recent results has been accepted for presentation at the 6th International Conference on Laser Spectroscopy (SICOLS) to be held in Interlaken, Switzerland, June 1983. They will also be presented in an invited paper at the 5th International Conference on Coherence and Quantum Optics in Rochester, June 1983.

Thus collision induced coherence is becoming a tool to study collisional effects on optical transitions with MHz resolution.

References

1. N. Bloembergen, M.C. Downer, and A. Bogdan, "Collision Induced Coherence in Four-Wave Light Mixing," in *Laser Spectroscopy V*, p. 157, edited by A.R.W. McKellan, T. Oka and B.P. Stoicheff, Springer, Heidelberg, 1981.

2. N. Bloembergen, M.C. Downer, and L.J. Rothberg, "Doppler Narrowing and Collision Induced Zeeman Coherence in Four-Wave Light Mixing," *Proc. 6th International Conference on Atomic Spectroscopy*, edited by I. Lindgren and S. Svanberg, Plenum, 1983.

II.2 Two-Photon Absorption Spectroscopy of Rare Earth Ions. M.C. Downer, A. Bivas, C.D. Cordero, and N. Bloembergen, Contract N00014-75-C-0648; Research Unit 5.

Experimental observation and theoretical analysis of the relative intensities and polarization dependence of fourteen two-photon transitions within the $4f^7$ configuration of the Gd^{3+} ion in LaF_3 and the isoelectronic Eu^{2+} ion in CaF_2 and SrF_2 have been completed.[1] The data deviate strongly

from predictions of a second order atomic theory of two-photon absorption. Most importantly, the selection rule $\Delta J \leq 2$ is violated and many transitions are anomalously strong. The results are explained by introducing third and fourth order terms in perturbation theory which take into account spin-orbit coupling and crystal field interaction among levels of the $4f^6 5d$ configuration, which serve as far off-resonant intermediate states. We discovered that the various higher order contributions could interfere with one another, leading to an unusual polarization dependence in the two-photon intensities, which has now been explained quantitatively. We also found that the intensities of individual fine structure, or crystal field, components could be explained consistently along with the integrated multiplet intensities. In fact, our measurements clarified a number of ambiguities in fine structure level assignments which had been left unresolved by energy level calculations. A brief report of the Gd^{3+} work has been published,[2] and comprehensive experimental and theoretical papers are in preparation.

In Eu^{2+}, in CaF_2, and SrF_2, sharp two-photon resonances from the $4f^7$ levels can be distinguished, which for one-photon absorption are hidden in the strong broad 5d bands, which lie low in energy for this ion. Numerous sharp transitions from the $f^7\ ^8S_{7/2}$ ground state to the $f^7\ ^6I$ and ^6D states have been observed for the first time, and energy level calculations have been performed for the new levels. The relative two-photon intensities again depend on higher order perturbations, which are even more important in Eu^{2+} than for Gd^{3+}. Strong evidence for a breakdown of the closure relation over the intermediate states, thus complicating the theoretical intensity calculations, has been found in the Eu^{2+} samples. These results were presented at the 12th International Conference on Quantum Electronics in Munich, June 1982.

2. H.M. Shen and R.W.P. King, "Experimental Investigation of the Rhombic EMP Simulator: Comparison with Theory and Parallel-Plate Simulator," *IEEE Trans. Electromagn. Compatibil.*, vol. EMC-24, 349-355, Aug. 1982.

IV.12 *Fields and Currents and Charges on Obstacles in a Parallel-Plate Simulator at Selected Frequencies and with Pulse Excitation*. H.M. Shen, R.W.P. King, and T.T. Wu, Contracts F29601-81-K-0010 and N00014-75-C-0648; Research Unit 10.

The parallel-plate Harvard model simulator has been investigated during the past several years in order to acquire a deep understanding of its properties as a means to improve its quality for EMP testing. The research was first carried out in the frequency domain. The electric field in the working volume and the associated distributions of current and charge on the metal plate have been measured at low, intermediate, and high frequencies. The results show that the simulator behaves quite differently with regard to the standing-wave ratio and its sensitivity to the termination in the different frequency ranges.[1] In particular, the intermediate frequency range includes the 'notch' phenomenon which was studied in detail in order to develop means for its elimination.[2] Current and charge densities induced on metal objects located at successively different points in a high standing-wave field in the simulator have been measured and compared with the corresponding quantities when the inducing field is a plane traveling TEM wave.[3] Significant differences are observed.

Since the structure of the Harvard model simulator is complicated, it is difficult to develop an adequate theory for the parallel and triangular plates as a unit. In order to understand the characteristics of the measured fields, a modified and simplified simulator, the rhombic-wire simulator, has been investigated (see heading IV.11). This incorporates the principal

properties of the metal-plate simulator and its structure is sufficiently simple to permit both a complete theoretical analysis and an experimental investigation. This study explains why the effects of the termination and the standing-wave ratio are different in the three frequency ranges. The calculation also shows the 'notch' at the intermediate frequency and reveals that it is caused by a combination of interference and reflection.

The investigation in the frequency domain was then extended to the time domain. The experimental results obtained for the rhombic simulator are very comprehensive.[4] They show that when the simulator is driven by a single voltage pulse, both the electric field in the simulator and the current along the metal wires consist of pulse sequences which include the incident pulse and reflected pulses from the terminals and from other parts of the simulator. The incident current pulse has a decaying amplitude and a relatively stable shape. The incident electric field is also a decaying pulse with almost the same width as the driving voltage pulse. Why does the width of the incident pulse not increase as it travels? Since it is excited by the current pulses as they travel along the rhombic wires with their very considerable length, time delays of the subpulses are quite different from those of a localized source. In order to explain the mechanism of excitation, a theory has been developed[5] which demonstrates that the 'time coincidences' of the subpulses play an important role in the formation of the complete electric-field pulse.

After this clarification of the characteristics of the rhombic simulator under pulse excitation, the consideration of the parallel-plate simulator could be resumed. The investigation of the Harvard model simulator under pulse excitation is very important. It reveals not only how the system actually behaves in an EMP test, but also provides a new tool for acquiring

information about the simulator which is difficult to obtain from CW measurements. Since the pulses reflected from different parts of or objects in the simulator are separated in time, it is possible to identify them in the complex sequence of observed pulses and then investigate them individually. This permits an individualized study of the effects caused by each object.

The properties of the parallel-plate Harvard model simulator have been studied experimentally in the time domain under single-pulse excitation.[6] Measurements have been made of the voltage at the driving point, the current and charge densities on the surfaces of the top plate, and the electric field between the plates in the simulator. It is shown that because of the shape and finite size of the simulator, the nature of the pulses observed at different locations is far from simple. The origin of the observed pulses is discussed with special reference to the more readily interpreted behavior of the rhombic simulator. In general, it may be said that the nature of the incident electric-field pulse in the working volume is reasonably like an incident plane pulse. This is of importance in the applications in full-sized simulators.

References

1. R.W.P. King and D.J. Blejer, "The Electromagnetic Field in an EMP Simulator at a High Frequency," *IEEE Trans. Electromagn. Compatibil.*, vol. EMC-21, 263-269, Aug. 1979.

2. R.W.P. King, D.J. Blejer, and T.T. Wu, "Standing Waves and Notches in an EMP Simulator and Their Reduction," *IEEE Trans. Electromagn. Compatibil.*, vol. EMC-23, 80-87, May 1981.

3. R.W.P. King, "Induced Charges on a Cylinder Excited by Standing and Traveling Waves in an EMP Simulator," *IEEE Trans. Electromagn. Compatibil.*, vol. EMC-24, 287-291, May 1982.

4. H.M. Shen, R.W.P. King, and T.T. Wu, "An Experimental Investigation of the Rhombic EMP Simulator under Pulse Excitation," *IEEE Trans. Electromagn. Compatibil.*, vol. EMC-25, 40-46, Feb. 1983.

5. H.M. Shen, R.W.P. King, and T.T. Wu, "Theoretical Analysis of the Rhombic Simulator under Pulse Excitation," *IEEE Trans. Electromagn. Compatibil.*, vol. EMC-25, 47-55, Feb. 1983.

6. H.M. Shen, R.W.P. King, and T.T. Wu, "An Investigation of the Parallel-Plate EMP Simulator with Single-Pulse Excitation," *IEEE Trans. Electromagn. Compatibil.* (submitted for publication).

IV.13 Solution for the Current Along a Cylindrical Antenna Driven by a Pulse Signal. H.M. Shen, Contract N00014-75-C-0648; Research Unit 10.

The evaluation of the distribution of current along a linear antenna has been a main subject of investigation in antenna theory. Once the current has been determined, the field and other relevant characteristics such as the radiation pattern and the input admittance can be calculated. Most of the work to date has been in the frequency domain. One approach to solve the current integral equation has made use of the peaking property of the kernel and an iterative procedure. In the time domain a corresponding integral equation for the current is easily obtained. However, when the attempt is made to solve this equation by the same procedure, the situation turns out to be quite different. When the system is driven by a voltage pulse, the current changes rapidly along the wire. At each location the current is zero or very small except while the pulse is passing. This behavior would seem to make the peaking property of the kernel no longer useful in solving for the current.

A new approximate approach for solving the integral equation for the current directly in the time domain has been developed.[1] After postulating a reasonable formal solution for the current pulse, using the 'time coincidence' property of the traveling pulse, and Laplace transforming the current integral equation, this is separated into three equations

(amplitude, shape, and tail equations) which can be solved sequentially. The first equation for the amplitude is solved separately. With the solution for the amplitude and the evaluation of a 'characteristic function' which appears in the second equation for the shape and represents the temporal characteristic of the system, the shape of the current is obtained by inverse Laplace transformation. The third equation for the tail is solved by using the iterative procedure after obtaining the main part of the current pulse. The final solution contains three parts: the steady-state current, the transient current, and the tail of the current pulse. This time-domain solution for the current has satisfactory quantitative accuracy (a relative error of less than 1%) with formal simplicity. It provides a physically meaningful representation.

Reference

1. H.M. Shen, "The Time Domain Solution of the Current Integral Equation," *IEEE Trans. Antennas Propagat.* (submitted for publication).

IV.14 Cylindrical and Conical Antennas as Probes for Measuring Electromagnetic Pulses. R.W.P. King, Contract N00014-75-C-0648; Research Unit 10.

In order to measure the components of the electromagnetic field, probes or sensors must be used that have known characteristics in their dependence on their dimensions and on the frequency. For use in the measurement of electro-magnetic pulses, the probe must be frequency-independent over the range of frequencies contained in the pulse. The electrically thin cylindrical dipole is a well-known and much used probe. Formulas and tables of its characteristics for both transmission and reception are generally

available over a very wide range of electrical lengths and radii. These formulas have been employed to determine the frequency dependence of the dipole.[1] It is shown that the cylindrical dipole is frequency-independent in the measurement of the time derivative of the electric field ($\partial E/\partial t$ in the time domain or ωE in the frequency domain) and not directly of the electric field. In the time domain, the electric field can be determined by means of an integration with respect to the time. In the frequency domain, the known characteristics of the cylindrical dipole make it useful for measuring the electric field. The possible application of the dipole as a calibration standard for testing other types of sensors is also illustrated.

Perhaps the most commonly used probes or sensors are conical in shape with variously rounded ends. They are quite well approximated by a cone with a spherical cap. Since biconical symmetry is violated when the two halves of a biconical antenna are separated to permit connection to a two-wire line, the conical antenna is most advantageously used as a monopole over a ground plane. In this configuration, it can be matched directly to a loading coaxial line with very small cross-sectional size. This preserves the conical symmetry to very close to the apex which, ideally, is a sharp point.

The generally theory of the conical antenna is well known, but explicit formulas even for the impedance require the solution of an infinite set of linear equations. Useful approximate solutions have been obtained for both narrow-angled and wide-angled cones. However, these are concerned specifically with the determination of the driving-point impedance and radiation field of driven antennas, and not with the effective length and current in the load of a receiving element excited by a plane wave incident at an

arbitrary angle. It is, nevertheless, possible to determine the frequency dependence of the current in the load of a conical receiving antenna by an application of the reciprocal theorem. A study of the electrically small, wide-angled, spherically capped conical monopole has been completed.[2] It is found to be a frequency-independent sensor for the time derivative of the electric field in the range $kL \approx k\ell(1+\Theta_0) \leq 1$ when the load is matched. Here, ℓ is the radius of the sphere and Θ_0 is half of the angle subtended by the cone. The properties of the conical monopole closely parallel those of the thin cylindrical monopole of length h in the corresponding range $kh \leq 1$, also with a matched load.

A possible advantage of the conical monopole over the thin cylinder is that its shape can be changed in order to modify somewhat the response near $k\ell = 1$. On the other hand, the thin cylinder is more readily available and is easily scaled to provide a wide range of sizes with the same properties. The conical shape is limited to the monopole over a ground plane since the bicone cannot be driven without separating the cones and violating the biconical geometry upon which the theoretical formulas depend.

References

1. R.W.P. King, "The Cylindrical Dipole as a Sensor or Probe," *IEEE Trans. Electromagn. Compatibil.*, vol. EMC-24, 364-367, Aug. 1982.

2. R.W.P. King, "The Conical Antenna as a Sensor or Probe," *IEEE Trans. Electromagn. Compatibil.*, vol. EMC-25, 8-13, Feb. 1983.

END

DATE
FILMED

8 — 83

DTIC